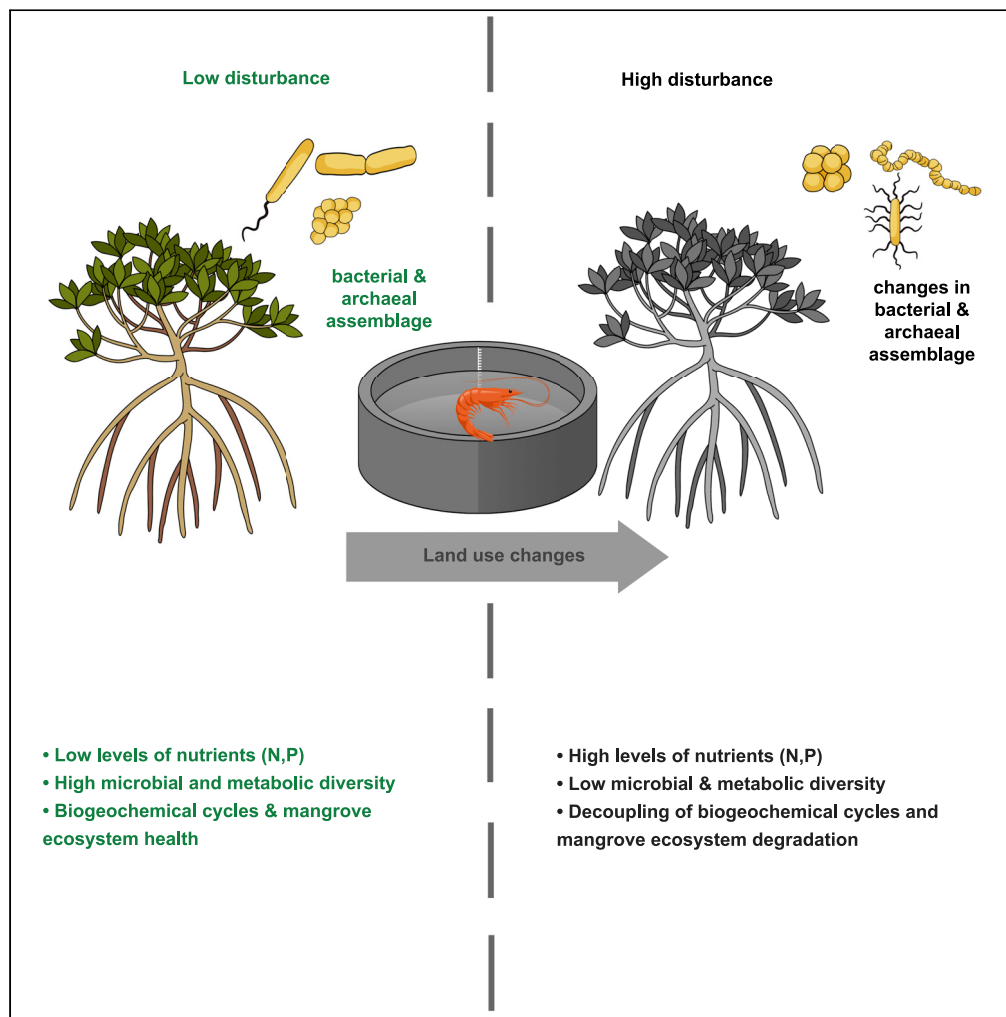## Article

Sensitivity of the mangrove-estuarine microbial community to aquaculture effluent

Natalia G. Erazo, Jeff S. Bowman

nerazo@ucsd.edu

HIGHLIGHTS

In near-intact mangrove forests, we observed the presence of nitrogen fixers

Calothrix could play a role in increasing nitrogen inventories via nitrogen fixation

Disturbed sites were correlated with increased nitrogen and reduction in diversity

Disturbed sites were dominated by nitrifiers, denitrifies, and sulfur-oxidizing bacteria

iScience

Article

Sensitivity of the mangrove-estuarine microbial community to aquaculture effluent

Natalia G. Erazo[1,3,4,*] and Jeff S. Bowman[1,2,3]

SUMMARY

Mangrove-dominated estuaries host a diverse microbial assemblage that facilitates nutrient and carbon conversions and could play a vital role in maintaining ecosystem health. In this study, we used 16S rRNA gene analysis, metabolic inference, nutrient concentrations, and $\delta^{13}C$ and $\delta^{15}N$ isotopes to evaluate the impact of land use change on near-shore biogeochemical cycles and microbial community structures within mangrove-dominated estuaries. Samples in close proximity to active shrimp aquaculture were high in NH_4^+, NO_3^- NO_2^-, and PO_4^{3-}; lower in microbial community and metabolic diversity; and dominated by putative nitrifiers, denitrifies, and sulfur-oxidizing bacteria. Near intact mangrove forests we observed the presence of potential nitrogen fixers of the genus *Calothrix* and order Rhizobiales. We identified possible indicators of aquaculture effluents such as *Pseudomonas balearica, Ponitmonas salivibrio,* family Chromatiaceae, and genus *Arcobacter*. These results highlight the sensitivity of the estuarine-mangrove microbial community, and their ecosystem functions, to land use changes.

INTRODUCTION

Mangrove forests are among the most productive ecosystems in the world, harbor significant biodiversity, and provide numerous ecosystem services (Ewel et al., 1998). These forests aid in the exchange of carbon and nutrients with the coastal marine environment (Robertson et al., 2011), with an estimated export of 10% of the marine dissolved organic matter to adjacent ecosystems (Dittmar and Lara, 2001). These forests act as carbon sinks by sequestering CO_2, help stabilize coastlines, and support coastal fisheries by acting as nursery grounds for a range of marine species (Kathiresan and Bingham, 2001). Despite their ecological and economic importance they have suffered severe losses in the past years (Duke et al., 2007). Although deforestation rates have declined (Friess et al., 2020), mangrove forests are still threatened by pollution, overextraction, conversion to aquaculture, agriculture, and the overall degradation of the environment (Lovelock et al., 2004; Reef et al., 2010; Friess et al., 2019).

A key driver of the reduction in mangrove forest area is the expansion of shrimp aquaculture. Within Ecuador, the expansion of aquaculture exceeds the global trend with deforestation rates higher than 80% (Hamilton and Lovette, 2015). Here, shrimp aquaculture has grown to a $1.3 billion industry by 2012 and represents the second largest component of the Ecuadorian economy after fossil fuels (Hamilton and Lovette, 2015). Shrimp aquaculture effluent is associated with the input of excess nutrients to adjacent coastal ecosystems; consequently, it can lead to changes in microbial community structure, biogeochemical cycles, and eutrophication (Maher et al., 2016; Rosentreter et al., 2018). Changes in nutrient fluxes can indirectly alter the redox state of the water column and sediment. This can shift mangrove forests from acting as sinks to sources of greenhouse gases such as CO_2, nitrous oxide, and methane (Maher et al., 2016).

Microorganisms (here meaning single-celled members of the domains bacteria, archaea, and eukarya) are a key component of the mangrove forest and are present in the sediment, the water column, and as biofilms on mangrove roots (Vazquez et al., 2000; Holguin et al., 2001). These microbes interact with mangroves as co-dependent ecosystem engineers and are responsible for many of the biogeochemical processes attributed to mangrove forests (Holguin et al., 2006; Reis et al., 2017; Shiau and Chiu, 2020). Mangrove forest productivity, for example, is dependent on the microbial recycling mechanisms that keep nitrogen and

[1]Scripps Institution of Oceanography, UC San Diego, 8622 Kennel Way, La Jolla, CA 92037, USA

[2]Center for Microbiome Innovation, UC San Diego, La Jolla, CA, USA

[3]Center for Marine Biodiversity and Conservation, UC San Diego, La Jolla, CA, USA

[4]Lead contact

*Correspondence: nerazo@ucsd.edu

Table 1. Environmental properties for high, intermediate, and low disturbed mangrove forests

Disturbance	Phosphate (μM)[a]	Nitrate+nitrite (μM)[a]	Ammonia (μM)[a]	Chlorophyll (μg L^{-1})[a]	δ^{13}C (range)[b]	δ^{15}N (range)[b]	Samples (n)[c, d, e]
Low	0.23 ± 0.23	0.46 ± 0.54	0.39 ± 0.36	11.52 ± 5.86	−18.45, −27.76	0.36, 11.08	89
Intermediate	0.33 ± 0.33	0.87 ± 0.46	1.77 ± 0.60	8.80 ± 2.58	−18.49, −29.00	0.54, 8.84	34
High	2.41 ± 1.01	9.91 ± 8.75	12.79 ± 7.50	30.75 ± 23.52	−27.01, −32.08	0.73, 5.86	29
p Value[f]	9.10 × 10^{11}	8.2 × 10^{-12}	2.20 × 10^{-16}	1.70 × 10^{-6}	–	–	–

[a]Mean value.
[b]Low and high values provided.
[c]Low disturbance (Cayapas-Mataje = 88, Muisne = 1).
[d]Intermediate disturbance (Cayapas-Mataje = 33, Muisne = 1).
[e]High disturbance (Muisne = 29).
[f]p Value (Kruskal-Wallis test).

other nutrients within the system (Alongi, 1994). Because of the dependence of ecosystem functions on microbes, microbes can be used as sensitive indicators of environmental change and stress.

The planktonic microbial community in mangrove forests has been understudied when compared with the sediment community (Gomes et al., 2011; Imchen et al., 2017; Zhang et al., 2017; Gong et al., 2019). In this study, we evaluated the impact of land use change (mangrove forest converted to aquaculture) on microbial community structure and key biogeochemical parameters in the water column. We tested the hypothesis that shrimp aquaculture facilities are correlated with increased nitrogen inputs, altered microbial structure, and alpha diversity. We identified specific microbial taxa that were differentially present between more and less perturbed sites associated with different levels of nutrient enrichment due to land use change. These taxa can be further developed as indicators of perturbation and mangrove forest health. The observed changes in the microbial community structure of the more and less disturbed sites highlighted the sensitivity of the mangrove forest to aquaculture effluent, with implications for coastal biogeochemical cycling and carbon and nitrogen subsidies to adjacent ecosystems.

RESULTS

Physicochemical properties

The disturbed sites (Muisne) were associated with higher levels of ammonia, nitrate + nitrite, phosphate, and chlorophyll a near aquaculture effluent sites (Figure 1). The mean concentrations were 2.41 ± 1.01 μmol L^{-1} for phosphate, 9.91 ± 8.75 μmol L^{-1} for nitrate + nitrite, 12.79 ± 7.50 μmol L^{-1} for ammonia, and 30.75 ± 23.52 μg L^{-1} for chlorophyll a (Table 1 and Figure 2). These biogeochemical parameters were significantly lower (Kruskal-Wallis test, p = 9.1 × 10^{-11}, 8.2 × 10^{-12}, 2.2 × 10^{-16}, 1.7 × 10^{-6}, respectively) in the low disturbance forest (Cayapas-Mataje) with values of 0.23 ± 0.23 μmol L^{-1} for phosphate, 0.46 ± 0.54 μmol L^{-1} for nitrate + nitrite, 0.39 ± 0.36 μmol L^{-1} ammonia, and 11.52 ± 5.86 μg L^{-1} chlorophyll a. Areas of intermediate disturbance were found around limited aquaculture facilities where the mean concentrations were 0.33 ± 0.33 μmol L^{-1} for phosphate, 0.87 ± 0.46 μmol L^{-1} for nitrate + nitrite, 1.77 ± 0.60 μmol L^{-1} for ammonia, and 8.80 ± 2.58 μg L^{-1} for chlorophyll (Table 1, Figure 2).

C and N isotope values ranged from −18.45 to −27.76‰ δ^{13}C in the low disturbed sites, −18.94 to −29.00‰ δ^{13}C in the intermediate disturbed sites, and −27.01 to −32.08‰ δ^{13}C in the high disturbed sites (Table 1, Figure 2). The δ^{15}N values ranged from 0.36 to 11.08‰ in the low disturbed sites, 0.54 to 8.84‰ in the intermediate disturbed sites, and 0.73 to 5.86‰ in the high disturbed sites (Table 1, Figure 2). The N* value for the high disturbed sites ranged from −43.68 to −4.44 μmol L^{-1}; for low and intermediate disturbance sites it ranged from −28.10 to 0.21 μmol L^{-1} (Figure 2). We identified higher N:P ratios associated with high disturbance and lower ratios with low disturbance sites, and we observed a negative correlation with genome size (Spearman's rho = −0.46, p = 9.3 × 10^{-8}) and 16S rRNA gene copy number (Spearman's rho = −0.5, p = 1.7 × 10^{-6}) (Figure 2). The taxa most associated with smaller predicted genomes were *Candidatus Dependentiae* (1.14 Mb), *Candidatus* Nasuia deltocephalinicola (1.12 Mb), and *Candidatus Pelagibacter* sp. IMCC9063 (1.28 Mb). The taxa most associated with larger predicted genomes were genera
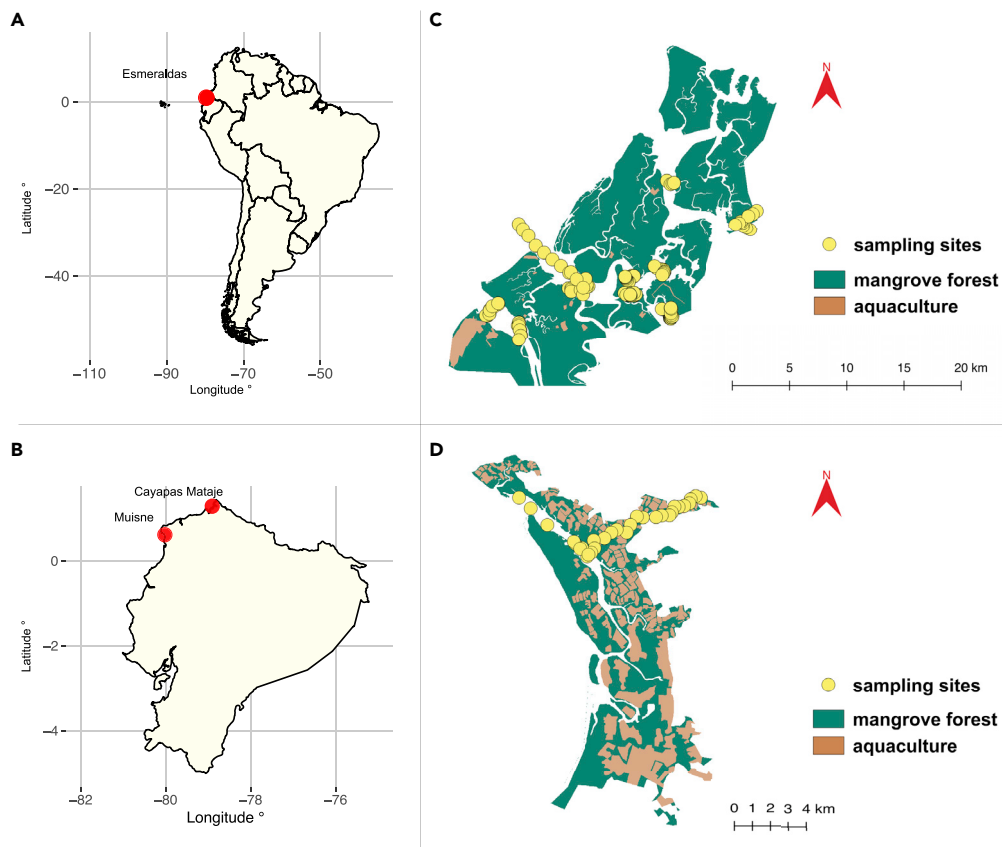
Figure 1. Map of study site in coastal Ecuador

(A) Study site in Esmeraldas, Ecuador, South America.

(B) Location of the two ecological reserves: Cayapas-Mataje (CM) and Muisne (M).

(C and D) (C) Map of land use changes in CM and (D) map of land use changes in M; green shows mangrove forest cover, pink shows shrimp aquaculture cover, and yellow circles show sampling locations. The base maps were generated from data obtained in Hamilton (2020).

Calothrix (12.05 Mb), *Oscillatoria acuminata* (7.80 Mb), *Moorea producens* PAL-8-15-08-1 (9.71 Mb), *Sandaracinus amylolyticus* (10.33 Mb), and *Singulisphaera acidiphila* (9.76 Mb).

Alpha diversity

For the bacterial community, the inverse Simpson's indicator of diversity was significantly lower in the highly disturbed sites when compared with the intermediate and low sites with mean $\pm$ SD values of 36.08 $\pm$ 26.41, 30.05 $\pm$ 17.56, and 56.73 $\pm$ 19.82 respectively, (Kruskal-Wallis, p = 3.5×10^{-9}) (Figure 3). The mean diversity for the archaeal community was 5.00 $\pm$ 1.34 for high, 6.38 $\pm$ 2.29 for intermediate, and 6.85 $\pm$ 2.87 for low disturbance sites, and low and intermediate disturbance sites had significant higher diversity than high disturbance sites (Kruskal-Wallis, p = 1.4×10^{-6}) (Figure 3). Alpha diversity for the archaeal community was lower than for the bacterial community. Low disturbance sites had higher diversity than intermediate disturbance sites for the bacterial community, but no difference was observed between low and intermediate sites for the archaeal community (Figure 3). We also evaluated the predicted metabolic diversity for the bacterial community; the mean metabolic diversity for low disturbance was 244.01 $\pm$ 8.72 (mean $\pm$ SD); for intermediate disturbance, was 235.22 $\pm$ 8.02; and for high disturbance, was 237.87 $\pm$ 9.29. The low disturbance sites had higher metabolic diversity (Kruskal-Wallis, p = 2.2×10^{-7}) when compared with intermediate and high disturbance sites.

Differentiated abundance of bacterial and archaeal communities and metabolic pathways

Unique reads are represented at the strain (closest completed genome or [CCG]) or clade level (closest estimated genome [CEG]) depending on the point of placement by paprica. The bacterial community
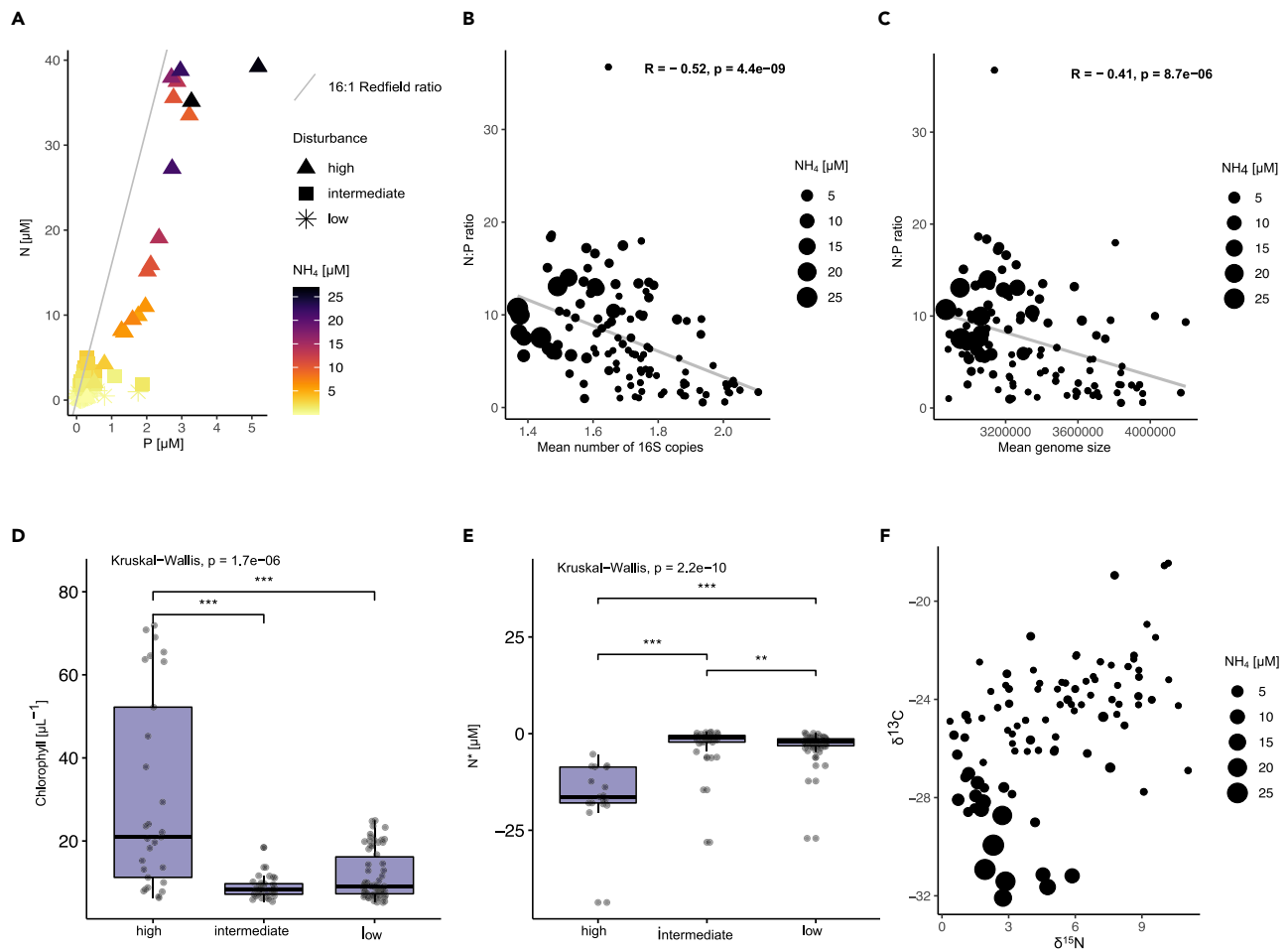
Figure 2. Biogeochemical and bacterial signatures

(A–C) (A) Nitrogen (ammonia and nitrate + nitrite) and phosphate species concentrations, (B) mean of genome size versus N:P ratio, (C) mean of number of 16S copies versus N:P ratio and Spearman's correlation.

(D and E) (D) N* value and (E) chlorophyll values of three levels of disturbance. Kruskal-Wallis test and p values with Dunn post-test. **p < 0.01, ***p < 0.001.

(F) $\delta^{13}C$ and $\delta^{15}N$ isotopic signatures.

composition was dominated by the class Actinobacteria: *Rhodoluna lacicola* (CEG), Actinobacteria bacterium IMCC26256 (CCG), *Acidimicrobium ferrooxidans* DSM 10331 (CCG); family Pelagibacteraceae: *Candidatus Pelagibacter* sp. IMCC9063 (CCG), *Candidatus Puniceispirillum marinum* IMCC1322 (CCG), *Candidatus Pelagibacter ubique* HTCC1062 (CCG); family Flavobacteriaceae: *Kordia* sp. SMS9 (CCG), *Owenweeksia hongkongensis* DSM 17368 (CCG); cyanobacteria: *Synechococcus* sp. WH 7803 (CCG); and family Rhodobacteraceae: *Thalassococcus* sp. S3 (CCG) and *Sulfitobacter* sp. AM1-D1(CCG). The archaeal community was dominated by the most abundant class Thermoplasmata: *Candidatus Methanomassiliicoccus intestinalis* Issoire-Mx1 (CCG), class Methanococci: Methanococcales (CEG), and phylum Thaumarchaeota (Figure S1).

Our DESeq2 results identified 333 amplicon sequence variants or ASVs that were significantly different between sites separated by level of disturbance. Here we focus on the top 60 most abundant differentially present ASVs that were significantly differentially present across our entire dataset (Figure 4). Members of *Chromatiaceae* bacterium 2141T.STBD.0c.01a (CCG) (p = 2.02 × 10⁻¹⁹), family Planctomycetes (CEG) (p = 1.62 × 10⁻⁹), genus *Delftia* (CEG) (p = 1.03 × 10⁻¹⁴), *Arcobacter nitrofigilis* DSM 7299 (CCG) (p = 1.31 × 10⁻⁷), *Steroidobacter denitrificans* (CEG) (p = 6.17 × 10⁻¹³), and *Pseudomonas balearica* DSM 6083 (CCG) (p = 2.52 × 10⁻⁸) were the most significantly most abundant taxa in the high disturbed site than in the low disturbed site. Cyanobacteria such as *M. producens* PAL-8-15-08-1 (CCG) (p = 2.45 × 10⁻⁷), order Nostocales (CEG) (p = 7.84 × 10⁻²⁹), and
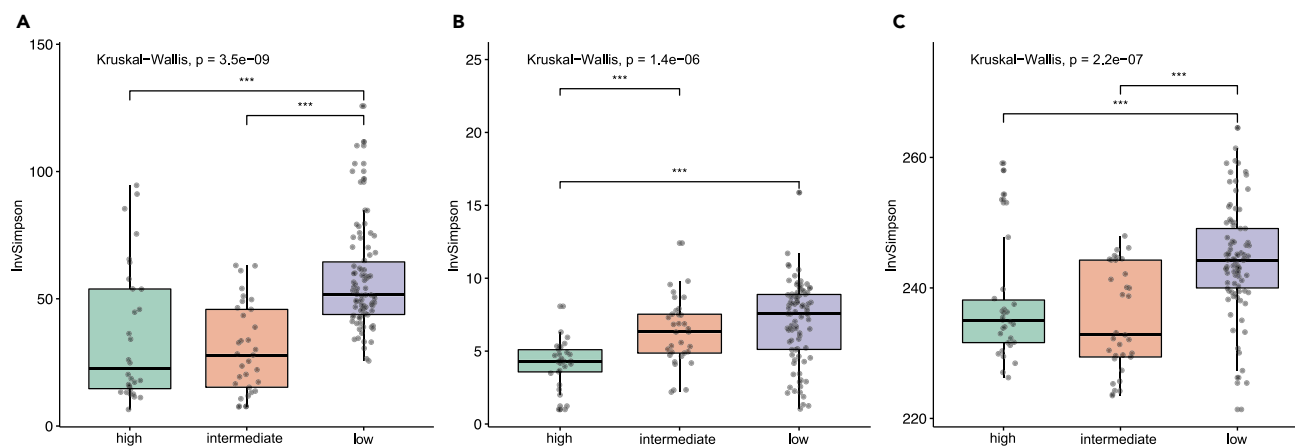
Figure 3. Alpha diversity

(A–C) (A) Bacterial community diversity, (B) archaeal diversity, and (C) metabolic diversity for the three levels of disturbance using InvSimpson metric. Kruskal-Wallis test and p values with Dunn post-test; ***p < 0.001.

Cyanobium gracile PCC 6307 (CCG) (p = 2.41 × 10^{-38}) were also more abundant in the high disturbed sites. The low disturbance sites were characterized by a higher abundance of SAR11 (CEG) (p = 2.17 × 10^{-14}), family Rhodobacteraceae (CEG) (p = 2.30 × 10^{-40}), family Flavobacteriaceae (CEG) (p = 8.26 × 10^{-28}), and genus *Methyloceanibacter* (CEG) (p = 1.42 × 10^{-8}). *Oscillatoria* species such as *Oscillatoria nigroviridis* PCC 7112 (CCG) (p = 9.12 × 10^{-7}) were more abundant in the low and intermediate disturbed sites as well as cyanobacteria *Calothrix* sp. NIES-4071 (CCG) (p = 1.79 × 10^{-20}) (Figure 4).

For domain archaea we identified a total of seven (CEG) taxa that were the most abundant and differentially present. *Candidatus Korarchaeota* (p = 1.09 × 10^{-13}) was associated with high disturbed samples. *Candidatus* Mancarchaeum acidiphilum (p = 4.28 × 10^{-40}), genus *Nitrosopumilus* (p = 2.92 × 10^{-68}), genus *Methanomassiliicoccus* (p = 5.08 × 10^{-28}), and genus *Methanococcales* (p = 3.79 × 10^{-56}) were more abundant in low disturbed sites (Figure 4).

A correspondence analysis (CA) of bacterial and archaeal community structures depicted the dissimilar relationship of samples for bacteria and archaea in terms of level of disturbance associated with aquaculture (Figure 5). For bacteria, the first axis explained 30.6%, and the second axis, 18.3%. The top contributing taxa to the difference were Betaproteobacteria (cos^2 = 0.86), *Acidothermus cellulolyticus* 11B (cos^2 = 0.83), and *S. denitrificans* (cos^2 = 0.91) (Figure 5). For the archaeal community, the first dimension accounted for 19.9% and the second dimension accounted for 11.8% of variability. Among the top contributors to the two dimensions were class Thermoplasmata (cos^2 = 0.61), *Candidatus Methanomassiliicoccus intestinalis* (cos^2 = 0.73), and *Candidatus* Mancarchaeum acidiphilum (cos^2 = 0.63) (Figure 5). The results of our ANOSIM test showed that the bacterial and archaeal communities were significantly different for low and high disturbance mangrove forests (R = 0.52 and p value = 0.001, R = 0.45 and p value = 0.001). We also observed clear association of location of samples with ammonia concentration in dimension 1 (Spearman's rho = 0.56, p = 1.4 × 10^{-10}) and dimension 2 (Spearman's rho = 0.54, p = 1.2 × 10^{-9}) for bacteria, and for archaea only dimension 2 showed a significant correlation (Spearman's rho = 0.49, p = 7.2 × 10^{-5}) (Figure S2).

A canonical correspondence analysis (CCA) was further performed to examine the relationships between metabolic pathways and environmental factors. This showed that the biogeochemical parameters associated with nitrogen species, phosphate, N:P, chlorophyll *a*, and δ^{13}C and δ^{15}N together accounted for 20% of the variability in the metabolic pathways. Nitrogen, phosphorus, and chlorophyll were factors that influenced the metabolic pathways in the high disturbance sites. The first dimension accounted for 26.1%, and the second dimension accounted for 9.1% of the variability. Here, the top contributors' predicted metabolic pathways of dimethylsulfoniopropionate (DMSP) degradation III methylation (cos^2 = 0.61) and glycine betaine (GBT) degradation I (cos^2 = 0.62) were associated with low and intermediate disturbance. Taxa associated with DMSP degradation III methylation were *Candidatus Puniceispirillum marinum* IMCC1322 and *Thalassococcus* sp. S3, and for GBT degradation, taxa were Alphaproteobacterium HIMB59, cyanobacteria, and Pelagibacteraceae. Other metabolic pathways with high contributions were arsenate
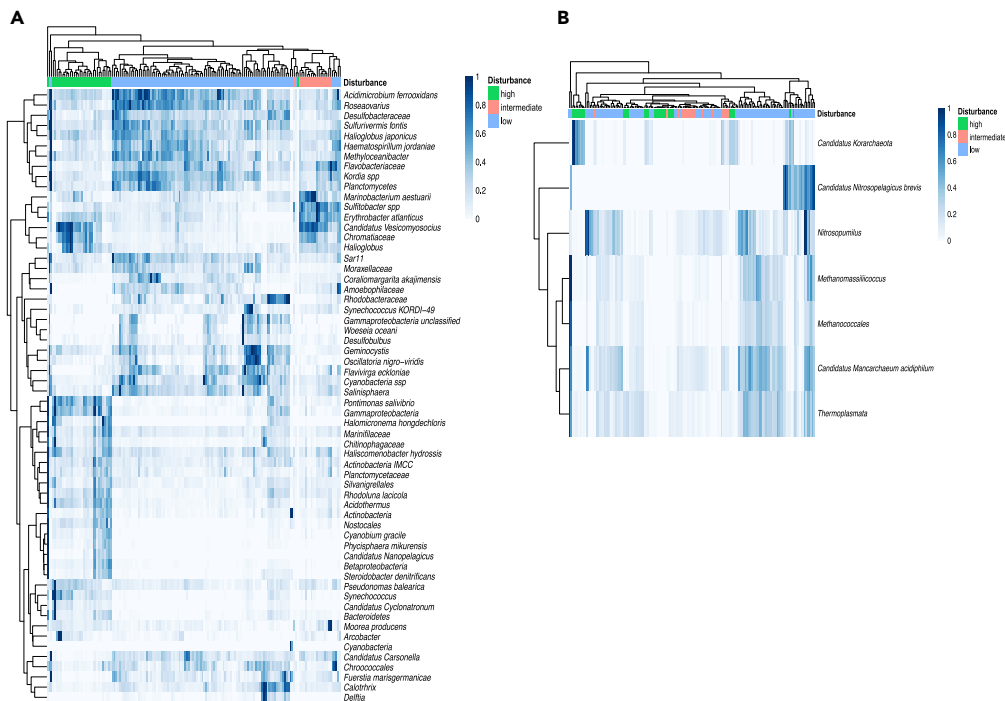
Figure 4. Microbial and archaeal signatures of disturbance

(A and B) (A) Differentially abundant bacterial taxa (top 60) in high, intermediate, and low disturbance result from DESeq2 analysis; (B) differentially abundant archaeal taxa result from DESeq2. Samples and taxa were clustered using Bray-Curtis dissimilarity distance.

detoxification (cos^2 = 0.75) and methylphosphonate degradation (cos^2 = 0.83), both associated with high disturbance sites (Figure 6). Taxa associated with these pathways were *Erythrobacter atlanticus* and *Candidatus* Puniceispirillum marinum IMCC1322 for arsenate detoxification and *Starkeya novella* DSM 506 (order Rizobiales) and *Oceanicola* sp. 3 for methylphosphonate degradation.

Weighted gene correlation network analysis

Weighted gene correlation network analysis (WGCNA) found clusters of highly correlated taxa across samples. We related these clusters to ammonia and nitrate + nitrite to better understand the impact of aquaculture effluent on microbial community structure. We identified eight major modules or subnetworks. Each module was assigned a particular color (Figure S3). The blue and pink modules were positively correlated with ammonia and nitrate + nitrite (blue: r = 0.64, p = 6.00×10^{-17}, pink: r = 0.86, p = 2×10^{-43}). The yellow module was negatively correlated with ammonia, nitrate, and nitrite (r = −0.42, p = 6.00×10^{-6}) (Figure S3). Taxa associated with the pink module (Figure S4) included *Sulfurivermis fontis* (CEG) (r = 0.90, p = 1.45×10^{-53}), *Actinobacteria* bacterium IMCC26256 (CCG) (r = 0.90, p = 9.62×10^{-53}), *Candidatus* Methylopumilus planktonicus (CEG) (r = 0.89, p = 1.98×10^{-50}) *Moorea producens* PAL-8-15-08-01 (CCG) (r = 0.89, p = 5.18×10^{-50}), *Phycisphaera mikurensis* NBRC 102666 (r = 0.85, p = 1.19×10^{-40}), *Cyanobium gracile* PCC 6307 (CCG) (r = 0.78, p = 7.76×10^{-30}), and *Steroidobacter denitrificans* (CEG) (r = 0.79, p = 2.31×10^{-30}). All these taxa were significantly correlated with ammonia, and with nitrate + nitrite (Table 2). Taxa most strongly associated with the blue module consisted of *C. bacterium* 2141T.STBD.0c.01a (CCG) (r = 0.49, p = 8.88×10^{-8}), *A. cellulolyticus* 11B (CCG) (r = 0.69, p = 3.37×10^{-20}), *S. denitrificans* (CEG) (r = 0.61, p = 3.62×10^{-14}), *Pontimonas salivibrio* (CEG) (r = 0.59, p = 1.52×10^{-15}), *M. producens* PAL-8-15-08-01 (CCG) (r = 0.69, p = 5.07×10^{-20}) (Table 2, Figure S4). The taxa that were most negatively correlated with ammonia in the yellow module were: *O. acuminata* PCC 6304 (CCG) (r = −0.34, p = 9.57×10^{-3}, *Synechococcus* sp. WH 7803 (CCG) (r = −0.49, p = 4.25×10^{-8}), *Candidatus pelagibacter* sp. IMCC9063 (CCG) (r = −0.37, p = 1.17×10^{-7}), and *Coraliomargarita akajimensis* DSM 45221 (CCG) (r = −0.36, p = 7.51×10^{-6}) (Table 2, Figure S4).

We further explored taxa that correlated with salinity to better understand the impact of tide on the microbial community structure. The red module was positively correlated with salinity (r = 0.47, p = 7.00×10^{-8})
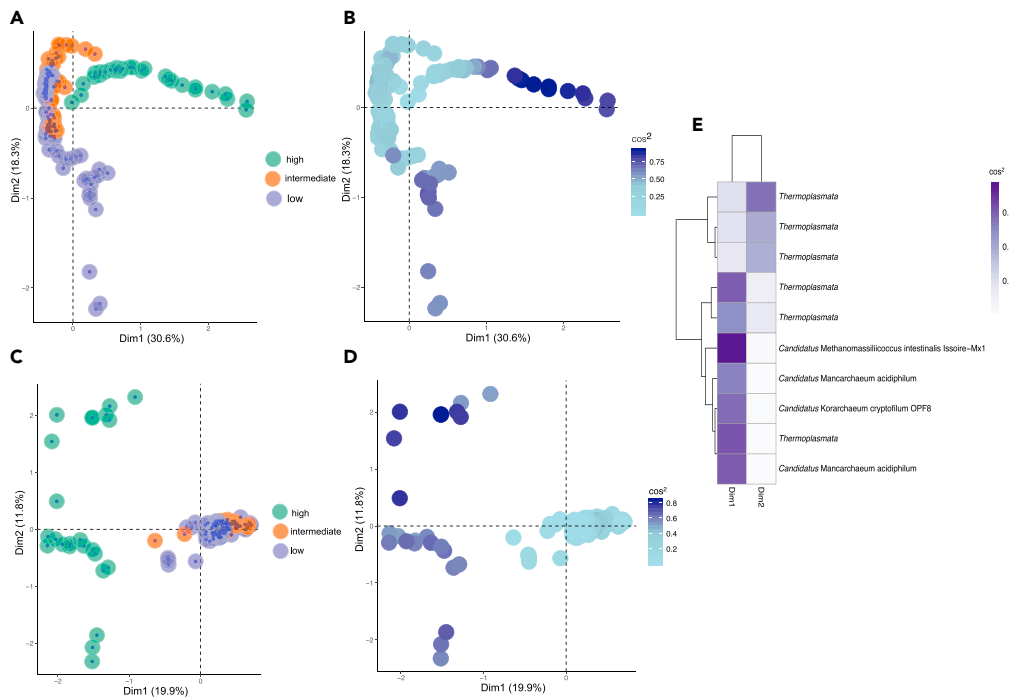
Figure 5. Bacterial and archaeal community structure

(A–E) Correspondence analysis (CA) ordination of (A) the bacterial community for samples that cluster in ordination space have similar community compositions, whereas those that are dispersed are less similar. (B) Square cosine components for samples; large value of cos2 shows a relatively large contribution to the total distance for bacterial community. (C) CA ordination for archaeal community. (D) Square cosine components for samples for archaeal community. (E) Contribution of top 10 taxa with highest cos2 values for archaeal community (see Figure S2).

(Figure S3). Taxa associated with the red module included *Acidimicrobium ferrooxidans* DSM 10331 (CCG) (r = 0.53, p = 8.19 × 10^{-10}), *Haliglobus japonicus* (CEG) (r = 0.52, p = 2.66 × 10^{-9}), *Synechococcus* sp. CC9605 (CCG) (r = 0.50, p = 2.28 × 10^{-8}), *Candidatus Puniceispirillum marinum* IMCC1322 (CCG)) (r = 0.47, p = 4.56 × 10^{-7}), and *Prochlorococcus marinus* str. MIT 9301 (r = 0.40, p = 1.98 × 10^{-4}) (Table 3).

We analyzed the Hellinger-transformed enzyme level output from paprica to better understand the enzymatic potential of those CEG and CCG that were correlated with ammonia. We found 35 enzymes associated with the nitrogen cycle (Figure 6). The enzyme nitrogenase EC 1.18.6.1 had a mean value of 0.23 ± 0.05 for the low disturbed sites, significantly higher than that in the intermediate (0.17 ± 0.06) and high (0.17 ± 0.05) disturbance sites (p = 1.2 × 10^{-10}) (Figure S5). Nitrate reductase EC 1.7.99.4 had a mean value of 0.23 ± 0.05 for low disturbance site, 0.45 ± 0.14 for intermediate disturbance site, and 0.44 ± 0.13 for high disturbance site, and the nitrate reductase value was significantly higher in the high disturbance sites (p = 8.7 × 10^{-14}). The same was observed with nitrate reductase NADH EC 1.7.1.4 with a mean of 0.13 ± 0.05 for low disturbed sites, 0.23 ± 0.14 for intermediate disturbance, and 0.23 ± 0.13 for highly disturbed sites (p = 2 × 10^{-15}) (Figures 6 andS5). The taxa that were associated with nitrogenase were *Methylocella silvestris* BL2, genus *Calothrix*, and *Synechococcus* sp. CC9605. For nitrate reductase members of the Betaproteobacteria, *Desulfococcus oleovorans* Hxd3, and *P. mikurensis* NBRC 102666 were found to contribute to enzyme abundance. The taxa that were associated with nitrate reductase NADH were *A. cellulolyticus* 11B and members of the Rhodobacteraceae (Table 4).

DISCUSSION

Mangrove forests are experiencing a high degree of perturbation through nutrient enrichment, pollution, and deforestation. Shrimp aquaculture effluent in particular is associated with the input of excess nutrients to mangrove forests. In this study we found that shrimp aquaculture effluent is associated with changes in microbial community structure with likely consequences for biogeochemical cycles and mangrove forest health. Previous work suggests that for intensive shrimp farming, 2.22 km^2 of mangrove forest is required
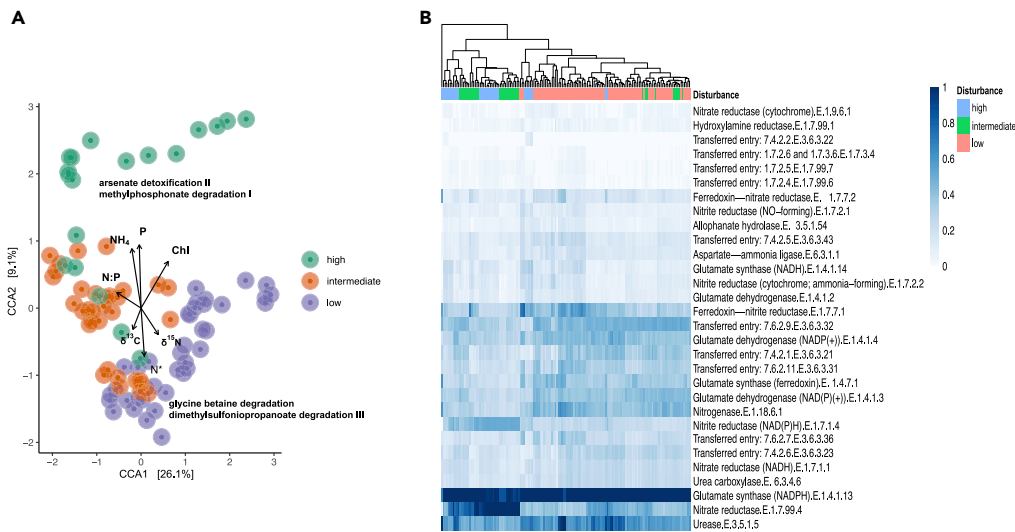
Figure 6. Metabolic pathways and nitrogen cycle enzyme indicators for levels of disturbance
(A) CCA ordination for metabolic pathways showing top four pathways with cos2 ranging from 0.6–0.8. Large value of cos2 shows a relatively large contribution to the total distance for bacterial metabolic prediction.
(B) Heatmap of key nitrogen cycle enzymes (Bray-Curtis distance) for the bacterial community (see Figure S5).

to remove effluent from one pond of 0.01 km^2, whereas 0.20 km^2 is required for less-intensive farming from one pond of 0.01 km^2 (Robertson and Phillips, 1995). As of 2014 in the Muisne region there were 20.47 km^2 of shrimp farms and 12.06 km^2 of mangrove forests, indicative of an intensive farming system. Cayapas-Mataje had 11.04 km^2 of shrimp aquaculture farms and 302.05 km^2 of mangrove forest, suggesting less intensive farming (Figure 1) (Hamilton, 2020). As the areal extent of shrimp aquaculture increases so does the volume of the effluent, elevating the flux of ammonia and nitrate to the surrounding ecosystem. Based on our observations we found that microbial communities in mangrove forests are significantly altered by this perturbation.

The bacterial communities in our mangrove systems were characterized by members of the Pelagibacteraceae, Flavobacteriaceae, Rhodobacteraceae, Actinobacteria, and cyanobacteria (Figure 4, Figure S1). The archaeal community was dominated by members of the Thermoplasmata, Thaumarchaeota, and Methanococcales (Figure 4, Figure S1). This was in accordance with other studies that have identified Rhodobacteraceae, SAR86 clade, Actinobacteria, and Flavobacteriaceae, and Thaumarchaeota as the most abundant taxonomic groups (Dhal et al., 2020). Rhodobacteraceae has been found to be dominant in mangrove-dominated estuaries, and members of this family are associated with marine phytoplankton blooms where they play a role in transformations of derived phytoplankton organic matter (Ghosh et al., 2010; Simon et al., 2017). The presence of Actinobacteria has been documented previously in mangrove ecosystems (Azman et al., 2015; Gong et al., 2019), and it has been suggested that they could play a role in carbon cycling by decomposing the plant biomass including refractory lignins (Scott et al., 2010). Thaumarchaeota are the most abundant archaea in the surface ocean (Santoro et al., 2015), and Thermoplasmata have been found in mangrove ecosystems (Zhang et al., 2019). Both these groups play an important role in the nitrogen cycle by carrying out the oxidation of ammonia in nitrification (Santoro et al., 2015; Zhang et al., 2019).

Both bacterial and archaeal communities were less diverse at our more disturbed sites. This pattern extended to predicted metabolic diversity (Figure 3). We hypothesize that this reduction in diversity could cause reductions in ecosystem functions. This has been observed in previous mangrove forest studies, for example, where lower microbial diversity was associated with a reduction in microbial productivity in sites with high levels of deforestation, sewage, and fishing activities (Carugati et al., 2018).

Our results showed differences in biogeochemical parameters between sites at varying levels of disturbance (Figure 2). In particular, nitrogen was a driver of the microbial community structure leading to segregation into three clusters of disturbance in the CA analysis based on our ANOSIM test and significantly

Table 2. Significant correlated taxa with ammonia and nitrate+nitrite result from WGCNA

Taxon	Map ID[a]	Module color	GS.Nitrogen[b]	p.GS.Nitrogen[c]
Thermogutta terrifontis[f]	0.87	Blue	0.74	6.35×10^{-25}
Acidothermus cellulolyticus 11B	0.94	Blue	0.69	3.37×10^{-20}
Oceanicola sp. D3	0.97	Blue	0.69	4.17×10^{-20}
Moorea producens PAL-8-15-08-1	0.82	Blue	0.69	5.07×10^{-20}
Moorea producens PAL-8-15-08-1	0.82	Blue	0.67	2.62×10^{-18}
Actinobacteria bacterium IMCC26256	0.88	Blue	0.62	8.57×10^{-15}
Steroidobacter denitrificans	0.91	Blue	0.61	3.62×10^{-14}
Aureitalea sp. RR4-38	0.92	Blue	0.61	5.70×10^{-14}
Pontimonas salivibrio	0.98	Blue	0.59	5.75×10^{-13}
Pontimonas salivibrio	0.98	Blue	0.59	1.52×10^{-15}
Acidothermus cellulolyticus 11B[f]	0.94	Blue	0.58	1.29×10^{-12}
Candidatus Xiphinematobacter sp. Idaho grape	0.88	Blue	0.58	1.80×10^{-12}
Synechococcus sp. CB0101	0.98	Blue	0.58	3.36×10^{-12}
Candidatus Cyclonatronum proteinivorum	0.87	Blue	0.57	9.00×10^{-12}
Candidatus Cyclonatronum proteinivorum	0.87	Blue	0.56	2.06×10^{-11}
Halioglobus pacificus	565	Blue	0.56	2.19×10^{-11}
Synechococcus sp. WH 8101	0.98	Blue	0.54	3.96×10^{-10}
Rhodoluna lacicola	0.98	Blue	0.53	1.58×10^{-9}
Actinobacteria bacterium IMCC26256	0.88	Blue	0.53	1.60×10^{-9}
Thiohalobacter thiocyanaticus	0.92	Blue	0.51	1.94×10^{-12}
Actinobacteria bacterium IMCC26256	0.88	Blue	0.50	9.01×10^{-12}
Chromatiaceae bacterium 2141T.STBD.0c.01a	0.95	Blue	0.49	8.88×10^{-8}
Wenzhouxiangella marina	0.98	Blue	0.48	1.48×10^{-7}
Thiolapillus brandeum	0.94	Blue	0.45	2.19×10^{-6}
Candidatus Puniceispirillum marinum IMCC1322	0.97	Blue	0.45	3.59×10^{-6}
Thermogutta terrifontis	0.87	Blue	0.44	4.27×10^{-6}
Candidatus Pelagibacter sp. IMCC9063	0.91	Blue	0.40	1.29×10^{-4}
Sulfurivermis fontis[d]	0.86	Pink	0.90	1.45×10^{-53}
Actinobacteria bacterium IMCC26256	0.88	Pink	0.90	9.62×10^{-53}
Candidatus Methylopumilus planktonicus	0.96	Pink	0.89	1.98×10^{-50}
Moorea producens PAL-8-15-08-1	0.82	Pink	0.89	5.18×10^{-50}
Owenweeksia hongkongensis DSM 17368	0.89	Pink	0.87	4.75×10^{-46}
Phycisphaera mikurensis NBRC 102666[e]	0.8	Pink	0.85	1.19×10^{-40}
Thermogutta terrifontis	0.87	Pink	0.85	2.24×10^{-40}
Candidatus Planktophila vernalis	0.95	Pink	0.85	9.07×10^{-40}
Actinobacteria bacterium IMCC26256	0.88	Pink	0.84	1.34×10^{-39}
Candidatus Xiphinematobacter sp. Idaho grape	0.88	Pink	0.83	7.44×10^{-37}
Candidatus Pelagibacter sp. IMCC9063	0.91	Pink	0.82	1.31×10^{-34}
Owenweeksia hongkongensis DSM 17368	0.89	Pink	0.81	3.97×10^{-33}
Syntrophus aciditrophicus SB	0.84	Pink	0.80	3.58×10^{-32}
Candidatus Pelagibacter sp. IMCC9063	0.92	Pink	0.79	1.73×10^{-31}
Phycisphaera mikurensis NBRC 102666[e]	0.8	Pink	0.79	1.89×10^{-30}

(Continued on next page)

Table 2. Continued

Taxon	Map ID[a]	Module color	GS.Nitrogen[b]	p.GS.Nitrogen[c]
Steroidobacter denitrificans	0.91	Pink	0.79	2.31×10^{-30}
Cyanobium gracile PCC 6307	0.98	Pink	0.78	7.76×10^{-30}
Cyanobium gracile PCC 6307	0.98	Pink	0.72	2.75×10^{-23}
Halioglobus japonicus	0.91	Pink	0.56	2.91×10^{-11}
Halomicronema hongdechloris C2206	0.9	Pink	0.53	7.85×10^{-10}
Thermogutta terrifontis	0.87	Pink	0.53	9.21×10^{-10}
Marinifilaceae bacterium SPP2	0.85	Pink	0.47	3.13×10^{-7}
Steroidobacter denitrificans	0.91	Pink	0.40	1.07×10^{-4}
Aureitalea sp. RR4-38	0.92	Yellow	−0.57	4.73×10^{-12}
Halioglobus pacificus	0.94	Yellow	−0.50	1.58×10^{-8}
Synechococcus sp. WH 7803	0.99	Yellow	−0.49	4.25×10^{-8}
Candidatus Methylopumilus planktonicus	0.96	Yellow	−0.47	4.55×10^{-7}
Flavobacteriaceae bacterium	0.91	Yellow	−0.45	2.36×10^{-6}
Thiolapillus brandeum	0.94	Yellow	−0.42	3.22×10^{-5}
Owenweeksia hongkongensis DSM 17368	0.89	Yellow	−0.39	2.45×10^{-4}
Thermogutta terrifontis	0.87	Yellow	−0.38	7.07×10^{-4}
Candidatus Pelagibacter sp. IMCC9063	0.92	Yellow	−0.37	1.17×10^{-3}
Coraliomargarita akajimensis DSM 45221	0.89	Yellow	−0.36	2.84×10^{-3}
Oscillatoria acuminata PCC 6304	0.81	Yellow	−0.34	6.15×10^{-3}
***Acidothermus cellulolyticus* 11B**[f]	0.94	Yellow	−0.34	9.57×10^{-3}

[a]Map ID phylogenetic classification. Value = 1 represents a perfect placement on the tree.
[b]GS = Pearson correlation to ammonia and nitrate + nitrite.
[c]p.GS = p-adjusted value (Bonferroni correction) for correlation to ammonia and nitrate+nitrite.
[d]Represents presence of nitrogenase enzyme EC.1.18.61.
[e]Represents presence of nitrate reductase enzyme EC.1.7.99.4.
[f]Represents presence of nitrate reductase enzyme EC.1.7.1.4.

correlated with ammonia concentrations (Figure 5, Figure S2). We note that the variance explained by the first and second dimensions in our ordination analyses is relatively low (30.6% and 19.9% for the bacterial and archaeal communities, respectively). We attribute this to the complexity associated with the mangrove ecosystem and the large number of physical, chemical, and biological factors that could impact changes in the microbial community.

We found a strong connection between N:P ratio and genome size among planktonic bacteria across study sites (Figure 2). Generally, smaller predicted genomes and lower 16S rRNA gene copy number was associated with higher N:P ratios, whereas larger predicted genomes and higher 16S rRNA gene copy number was associated with lower N:P ratios. The differences in genome sizes between communities associated with different levels of disturbance suggest differing ecological strategies. Studies suggest that generalists possess larger genomes in contrast to the smaller genomes in more specialized microbes (Sriswasdi et al., 2017; Willis and Woodhouse, 2020). This falls from the generalist requirement for a larger gene repertoire to boost activity in multiple environmental conditions and to cope with different stressors associated with a broad physicochemical niche (such as low levels of nitrogen and tidal fluctuations in mangrove-dominated estuaries). The low disturbance sites showed a higher metabolic diversity and larger genomes, which we interpret as a more generalist microbial community. Taxa with larger genomes included Planctomycetes such as *Singulisphaera acidiphila*. This taxon has been found in other wetland ecosystems (Kulichevskaya et al., 2008; Dedysh and Ivanova, 2019), and it has been shown to play an important role in degradation of plant-derived polymers such as pectin and xylan (Dedysh and Ivanova, 2019). The *S. acidiphila* genome encodes several dozen proteins that do not belong to any of the currently carbohydrate-active enzymes, but the enzymes display a distant relationship to glycosyltransferases and carbohydrate esterases, suggesting that this taxon has a diverse glycolytic and carbohydrate metabolic potential (Dedysh and Ivanova, 2019). Other taxa included *Sandaracinus amylolyticus*. This taxon has been found in association with plant

Table 3. Significant correlated taxa with salinity result from WGCNA

Taxon	Map ID[a]	Module color	GS.Salinity[b]	p.GS.Salinity[c]
Acidimicrobium ferrooxidans DSM 10331	0.94	Red	0.53	8.19×10^{-10}
Kordia sp. SMS9	0.91	Red	0.53	1.49×10^{-9}
Halioglobus japonicus	0.93	Red	0.52	2.66×10^{-9}
Synechococcus sp. CC9605	1.00	Red	0.50	2.28×10^{-8}
Synechococcus sp. RCC307	1.00	Red	0.47	4.36×10^{-7}
Candidatus Puniceispirillum marinum IMCC1322	0.98	Red	0.47	4.56×10^{-7}
Salipiger profundus	0.82	Red	0.46	8.37×10^{-7}
Halioglobus pacificus	0.95	Red	0.46	1.02×10^{-6}
Roseovarius mucosus	0.96	Red	0.44	7.04×10^{-6}
Acidimicrobium ferrooxidans DSM 10331	0.82	Red	0.41	9.08×10^{-5}
Candidatus Pelagibacter ubique HTCC1062	1.00	Red	0.40	1.10×10^{-4}
Owenweeksia hongkongensis DSM 17368	0.89	Red	0.40	1.64×10^{-4}
Prochlorococcus marinus str. MIT 9301	1.00	Red	0.40	1.98×10^{-4}
Synechococcus sp. KORDI-100	1.00	Red	0.39	2.07×10^{-4}
Sulfurivermis fontis	0.87	Red	0.39	3.93×10^{-4}

[a]Map ID phylogenetic classification. Value = 1 represents a perfect placement on the tree.
[b]GS = Pearson correlation to salinity.
[c]p.GS = p-adjusted value (Bonferroni correction) for correlation to salinity.

residues (Mohr et al., 2012), in coral ecosystems (Rubio-Portillo et al., 2016), and it is known to survive in poor nutrient conditions by developing desiccation-resistant spores (Mohr et al., 2012).

We also observed larger genomes in cyanobacteria including members of the genus *Calothrix*, genus *Oscillatoria*, and *M. producens* PAL-8-15-08-1. Cyanobacteria are known to have large genomes with low coding density and a high level of gene duplication; it has been proposed that the large non-protein-coding sequences contribute to the genome expansion and metabolic flexibility observed in diazotrophs (nitrogen fixers) that are associated with nitrogen-limited environments (Sargent et al., 2016). The high diversity of cyanobacteria observed in mangrove ecosystems suggests that they play a key role in the ecosystem. Relevant functions associated with cyanobacteria include nitrogen and carbon fixation and the production of herbivory-defense molecules and plant growth-promoting substances (Alvarenga et al., 2015).

In the disturbed sites the parasite *C. Dependentiae* accounted for much of the decrease in genome size. Studies have found that *C. Dependentiae* infects a wide range of protists, including heterotrophs and phytoplankton (Deeg et al., 2019). Other studies have shown that *C. Dependentiae* is associated with free-living ameba, suggesting that it could be an endosymbiont (Delafont et al., 2015). *C. Dependentiae* has very limited metabolic capability, lacks complete biosynthetic pathways for various essential cellular building blocks, and has protein motifs to facilitate eukaryotic host interactions (Yeoh et al., 2016; Deeg et al., 2019). *C. Nasuia deltocephalinicola* was also identified as having a small genome. *C. Nasuia deltocephalinicola* is an obligate symbiont of plant phloem-feeding pest insects, and its main role is to provide essential amino acids that the host can neither synthesize nor obtain in sufficient quantities from a plant diet (Bennett and Moran, 2013).

The increase in the concentration of nitrogen species associated with aquaculture effluent could further select for specialist microbes with reduced metabolic potential and lower diversity in nitrogen-processing enzymes. Our nitrogen isotope values are consistent with this, showing reduced variability for the highly disturbed sites (Table 1, Figure 2). Previous work in mangrove systems (Bernardino et al., 2018) associated reduced isotopic variability with a loss of trophic diversity. Higher variability in stable carbon isotopes has also been observed in salt marshes due to contribution dominated by allochthonous material derived from the phytoplankton community (Boschker et al., 1999). The larger variation in the isotopic signal observed in the low and intermediate disturbance sites suggests that these pristine systems contain a more diverse

Table 4. Number of enzymes copies for nitrogenase and nitrate reductase enzymes and top 10 associated taxa

Taxon	Nitrogenase EC.1.18.6.1	Nitrate reductase EC.1.7.99.4	Nitrate reductase NADH EC.1.7.1.4
Methylocella silvestris BL2	16,984	4,246	0
Genus *Calothrix*	15,186	3,796	0
Synechococcus sp. CC9605	38,937	0	0
Family Rhodobacteraceae	0	0	1,273
Oscillatoria nigroviridis PCC 7112	0	5,418	5,418
Acidothermus cellulolyticus 11B	0	0	23,205
Phycisphaera mikurensis NBRC 102666	0	8,288	0
Rhodopirellula baltica SH 1	0	10,956	21,912
Desulfococcus oleovorans Hxd3	0	4,773	0
Class Betaproteobacteria	0	17,102	0

trophic food web as result of a wide range of metabolic and fixation pathways, and environmental conditions in the mangrove-estuarine ecosystem (Boschker and Middelburg, 2002).

The low N:P ratios we observed in the low disturbance sites suggest that the system is N limited. Pristine mangrove forests tend to be N limited, although nutrients are not uniformly distributed within the mangrove ecosystem and they can switch from N to P limitation. It has been shown that mangrove trees within fringe and tidally exposed zones tend to be N limited (Feller et al., 2003). One way mangrove trees cope with N limitation is through associations with diazotrophs that play a crucial role in N cycling within the mangrove forest (Holguin et al., 1992). Here we showed that the biological nitrogen fixation signal, confirmed by the N* value (the linear combination of nitrate and phosphate that eliminates the effect of nitrification; thus, the remaining variability can be explained by nitrogen fixation and denitrification) (Gruber and Sarmiento, 1997) and nitrogenase EC.1.18.6.1 abundance, were higher at low disturbance sites in contrast to high disturbance sites (Figures 2, 6, and S5). The microbial denitrification signal was further confirmed by negative N* values in the highest disturbance sites (Figure 2) (Gruber and Sarmiento, 1997). Because excess nitrate is being introduced into the system via aquaculture effluent, we expect denitrification rates to be high. Conversely, the lowest disturbance sites have a slight positive N* consistent with our identification of putative diazotrophs such as genus *Calothrix,* genus *Oscillatoria,* and taxa of the order Rhizobiales such as *M. silvestris* (Essien et al., 2008; Liu et al., 2019).

GBT degradation I was one of the major pathways contributing to the differences observed between low and high disturbed sites (Figures 6 and S3). GBT is an important source of nitrogen in oligotrophic systems, acts as an organic osmolyte, and plays an important role in phytoplankton-bacteria interactions (Becker et al., 2019; Jones et al., 2019; Zecher et al., 2020). The intertidal coastal mangrove ecosystem experiences daily fluctuations in a range of environmental conditions, including water levels and salinity. Organisms living in this dynamic environment cope with changing environmental conditions by synthesizing a range of organic and inorganic osmolytes including GBT. The results from WGCNA showed that Pelagibacteraceae taxa correlated with salinity (Table 3) and primary contributors of the GBT degradation I pathway. This suggests that osmolyte production is an important adaptation to salinity intrusions from oceanic waters into the mangrove environment, and GBT could be an additional pool of organic N within this system.

Shrimp aquaculture impacts the water quality in adjacent mangrove forests by creating eutrophic conditions that can lead to anoxia. Eutrophic conditions were evident through high levels of nutrients and chlorophyll *a* (Figure 2, Table 1). Although we did not measure oxygen concentrations, we observed taxa indicative of hypoxic or anoxic conditions. These included purple sulfur bacteria (PSB), such as family Chromaticeae, and sulfur-oxidizing bacteria (SOB), such as genus *Sulfurivermis* (Figure 4, Table 2). PSB use sulfide, elemental sulfur, and thiosulfate as electron donors in anoxygenic photosynthesis and have been shown to play an important role in regime shifts from oxygenated to anoxic conditions (Diao et al., 2018). PSB flourish in micro-aerobic conditions oxidizing sulfide into sulfate (Diao et al., 2018). As the oxygen influx is reduced below a critical threshold, sulfate-reducing bacteria (SRB) and PSB can take over and outcompete the SOB. This suggests a more anoxic regime in the high disturbance site, allowing for PSB groups and SRB to become more abundant.

Based on our WGCNA analysis we also found nitrate-reducing bacteria (NRB)—indicative of reduced oxygen availability—that strongly correlated with the level of ammonia, nitrate, and nitrite. Putative NRB taxa included *P. mikurensis* and *S. denitrificans* (Table 2). In addition, we also saw a microbial signature associated with dissimilatory nitrate reduction to ammonium (DNRA) with the presence of genus *Acidothermus*, and anaerobic ammonium oxidation (annamox) with the presence of Planctomycetes *(Thermogutta terrifontis)* (Table 2); the presence of the genes involved in these pathways (denitrification, annamox, DNRA) were inferred by paprica, although further work is needed to confirm the presence and activity of these enzymes. Overall, as nitrate and ammonia inputs increased with aquaculture effluent the relative abundance of NRB increased.

We identified specific microbes that can be used as sensitive indicators of aquaculture impacts. These included *P. balearica* (Figure 4), which has been associated with other contaminated wetland systems, suggesting that this taxon could be a potential bio-indicator of a disturbed mangrove ecosystem (Salvà-Serra et al., 2017). Similar studies have also identified aquaculture effluent as a source of pathogens to the coastal ecosystem (Garren et al., 2009). In the disturbed site we saw the presence of members of the genus *Arcobacter* (Figure 4). These bacteria have been identified in coral systems exposed to aquaculture effluents, and have been associated with feces (human, porcine, and bovine) and with sewage-contaminated waters (Garren et al., 2009). PSB taxa such as family Chromaticeae have also been shown to be potential bio-indicators for anthropogenic contamination associated with other agriculture effluent systems (Mohd-Nor et al., 2018). *P. salivibrio* in the order Micrococcales was elevated at the disturbed sites. This taxon has been isolated from high-salinity systems and aquaculture farms (Jang et al., 2013); high salinity levels have been associated with shrimp aquaculture effluent due to high evaporation in the ponds (Barraza-Guardado et al., 2013). Previous studies have shown that taxa in the Micrococcales order are part of the core microbiome signal in shrimp ponds (Chen et al., 2017). Thus, *P. salivibrio* is a sensible indicator of shrimp aquaculture effluent. Further work is needed to establish robust spatiotemporal baselines of microbial indicators of aquaculture to effectively monitor biogeochemical changes and health of the mangrove forests.

Aquaculture could impact the health of mangrove ecosystems involving the direct loss of mangrove forests, effluent associated with high levels of nutrients, and the development of anoxic and sulfuric water conditions (Robertson and Phillips, 1995). Aquaculture effluent released into mangrove forests may be sequestered and processed by bacteria. However, processing efficiency could change with increasing input. High organic loadings, for example, may shift the balance from aerobic to anaerobic systems (Lønborg et al., 2020). Anaerobic systems are less efficient in nutrient cycling. The signals of SOB, SRB, denitrifiers, and potential pathogenic taxa associated with the perturbed site suggest that aquaculture effluent is playing a role in shifting the microbial community to a more pathogenic and less nutrient efficient community that could impact the health of the mangrove forest.

Conclusion

In this study, we showed the impacts of aquaculture effluent on the microbial community structure in mangrove forests and identified microbial signals associated with NRB, PSB, and SRB taxa that could have impacts in nutrient cycling. The high level of nutrients in the perturbed sites were associated with changes in microbial community structure that could impact ecosystem functions. In the low disturbance sites, we saw that the presence of *Calothrix* species and nitrogen fixers could be important in increasing nitrogen inventories via nitrogen fixation. Denitrification reduces excess inorganic nitrogen concentration, and in the highly disturbed sites we saw the presence of NRB-associated microbes. Nutrient cycling in mangrove habitats is a balance between nutrient inputs, availability, and internal cycling, and the changes in microbial community structure we see in disturbed sites could be indicators of biogeochemical changes. The results of the study highlight the sensitivity of the mangrove-estuarine microbial community to aquaculture effluent, and the impacts of land use changes could be amplified by climate change such as changing precipitation patterns, heat, and rising sea level with severe consequences for the ecosystem.

Limitations of the study

Our analysis was based on comparison between sites of low, intermediate, and high disturbance in two mangrove systems in coastal Ecuador. Although ammonia concentration is a good proxy for disturbance from shrimp aquaculture effluent, quantification of land use changes, and the hydrological connections between aquaculture facilities and our sampling sites was beyond the scope of the current work. We

considered salinity, macronutrient concentrations, and isotopes in our analysis, but anticipate that other variables not considered here are contributing to differences in microbial community structure. These include physical processes such as tides and hydrology. The complexity of these environments is evident in our CCA and CA analyses, which capture a relatively small amount of variability in the first two dimensions (see discussion section). Other limitations of note are typical of microbial community structure analyses. These include primer bias and a dependence on relative rather than absolute abundance.

Resource availability

Lead contact

Further information and requests for resources should be directed to and will be fulfilled by the lead contact, Natalia Erazo (nerazo@ucsd.edu).

Materials availability

This study did not generate new unique reagents.

Data and code availability

The data that support the findings of this study and sequences were submitted to the NCBI sequence read archive (SRA) under BioProject ID: PRJNA633714. Code for analysis is available on github repository: https://github.com/galud27.

METHODS

All methods can be found in the accompanying Transparent methods supplemental file.

SUPPLEMENTAL INFORMATION

Supplemental information can be found online at https://doi.org/10.1016/j.isci.2021.102204.

AUTHOR CONTRIBUTIONS

Conceptualization, N.G.E. and J.S.B.; Methodology, N.G.E. and J.S.B; Investigation, N.G.E. and J.S.B; Writing – Original Draft, N.G.E.; Writing – Review & Editing, J.S.B.; Funding Acquisition and Supervision, J.S.B.

DECLARATION OF INTERESTS

The authors declare no competing interests.

REFERENCES

Alongi, D.M. (1994). The role of bacteria in nutrient recycling in tropical mangrove and other coastal benthic ecosystems. Hydrobiologia *285*, 19–32.

Alvarenga, D.O., Rigonato, J., Branco, L.H.Z., and Fiore, M.F. (2015). Cyanobacteria in mangrove ecosystems. Biodivers. Conserv. *24*, 799–817.

Azman, A.S., Othman, I., Velu, S.S., Chan, K.G., and Lee, L.H. (2015). Mangrove rare actinobacteria: taxonomy, natural compound, and discovery of bioactivity. Front.Microbiol. *6*, 856.

Barraza-Guardado, R.H., Arreola-Lizárraga, J.A., López-Torres, M.A., Casillas-Hernández, R., Miranda-Baeza, A., Magallón-Barrajas, F., and Ibarra-Gámez, C. (2013). Effluents of shrimp farms and its influence on the coastal ecosystems of Bahía de Kino, Mexico. Sci.WorldJ. *2013*, 306370.

Becker, J.W., Hogle, S.L., Rosendo, K., and Chisholm, S.W. (2019). Co-culture and biogeography of Prochlorococcus and SAR11. ISME J. *13*, 1506–1519.

Bennett, G.M., and Moran, N.A. (2013). Small, smaller, smallest: the origins and evolution of ancient dual symbioses in a phloem-feeding insect. Genome Biol. Evol. *5*, 1675–1688.

Bernardino, A.F., Gomes, L.E.O., Hadlich, H.L., Andrades, R., and Correa, L.B. (2018). Mangrove clearing impacts on macrofaunal assemblages and benthic food webs in a tropical estuary. Mar. Pollut.Bull. *126*, 228–235.

Boschker, H.T.S., de Brouwer, J.F.C., and Cappenberg, T.E. (1999). The contribution of macrophyte-derived organic matter to microbial biomass in salt-marsh sediments: stable carbon isotope analysis of microbial biomarkers. Limnol. Oceanogr. *44*, 309–319.

Boschker, H.T., and Middelburg, J.J. (2002). Stable isotopes and biomarkers in microbial ecology. FEMS Microbiol. Ecol. *40*, 85–95.

Carugati, L., Gatto, B., Rastelli, E., Lo Martire, M., Coral, C., Greco, S., and Danovaro, R. (2018). Impact of mangrove forests degradation on biodiversity and ecosystem functioning. Sci. Rep. *8*, 13298.

Chen, W.-Y., Ng, T.H., Wu, J.H., Chen, J.W., and Wang, H.C. (2017). Microbiome dynamics in a shrimp grow-out pond with possible outbreak of acute hepatopancreatic necrosis disease. Sci. Rep. *7*, 9395.

Dedysh, S.N., and Ivanova, A.A. (2019). Planctomycetes in boreal and subarctic wetlands: diversity patterns and potential ecological functions. FEMS Microbiol. Ecol. *95*, 227.

Deeg, C.M., Zimmer, M.M., George, E.E., Husnik, F., Keeling, P.J., and Suttle, C.A. (2019). Chromulinavorax destructans, a pathogen of microzooplankton that provides a window into the enigmatic candidate phylum dependentiae. PLoS Pathog. *15*, e1007801.

Delafont, V., Samba-Louaka, A., Bouchon, D., Moulin, L., and Héchard, Y. (2015). Shedding light on microbial dark matter: a TM6 bacterium as natural endosymbiont of a free-living amoeba. Environ.Microbiol. Rep. *7*, 970–978.

Dhal, P.K., Kopprio, G.A., and Gärdes, A. (2020). Insights on aquatic microbiome of the Indian Sundarbans mangrove areasJ.-S. Hwang, ed. *15*, e0221543.

Diao, M., Huisman, J., and Muyzer, G. (2018). Spatio-temporal dynamics of sulfur bacteria during oxic-anoxic regime shifts in a seasonally stratified lake. FEMS Microbiol. Ecol. *94*, 40.

Dittmar, T., and Lara, R.J. (2001). Do mangroves rather than rivers provide nutrients to coastal environments south of the Amazon River? Evidence from long-term flux measurements. Mar. Ecol. Prog.Ser. *213*, 67–77.

Duke, N.C., Meynecke, J.-O., Dittmann, S., Ellison, A.M., Anger, K., Berger, U., Cannicci, S., Diele, K., Ewel, K.C., Field, C.D., et al. (2007). A world without mangroves? Science *317*, 41b–42b.

Essien, J.P., Antai, S.P., and Benson, N.U. (2008). Microalgae biodiversity and biomass status in Qua Iboe Estuary mangrove swamp, Nigeria. Aquat. Ecol. *42*, 71–81.

Ewel, K.C., Twilley, R.R., and Ong, J.E. (1998). Different kinds of mangrove forests provide different goods and services. Glob. Ecol. Biogeogr. Lett. *7*, 83.

Feller, I.C., McKee, K.L., Whigham, D.F., and O'Neill, J.P. (2003). Nitrogen vs. phosphorus limitation across an ecotonal gradient in a mangrove forest. Biogeochemistry *62*, 145–175.

Friess, D.A., Rogers, K., Lovelock, C.E., Krauss, K.W., Hamilton, S.E., Lee, S.Y., Lucas, R., Primavera, J., Rajkaran, A., and Shi, S. (2019). 'The state of the world's mangrove forests: past, present, and future'. Annu. Rev. Environ. Resour. *44*, 89–115.

Friess, D.A., Yando, E.S., Abuchahla, G.M.O., Adams, J.B., Cannicci, S., Canty, S.W.J., Cavanaugh, K.C., Connolly, R.M., Cormier, N., and Dahdouh-Guebas, F. (2020). Mangroves give cause for conservation optimism, for now. Curr. Biol. *30*, R153–R154.

Garren, M., Raymundo, L., Guest, J., Harvell, C.D., and Azam, F. (2009). Resilience of coral-associated bacterial communities exposed to fish farm effluent. PLoS One *4*, e7319.

Ghosh, A., Dey, N., Bera, A., Tiwari, A., Sathyaniranjan, K.B., Chakrabarti, K., and Chattopadhyay, D. (2010). Culture independent molecular analysis of bacterial communities in the mangrove sediment of Sundarban, India. Saline Syst. *6*, 1.

Gomes, N.C., Cleary, D.F., Calado, R., and Costa, R. (2011). Mangrove bacterial richness. Commun.Integr. Biol. *4* (4), 419–423.

Gong, B., Cao, H., Peng, C., Perčulija, V., Tong, G., Fang, H., Wei, X., and Ouyang, S. (2019). High-throughput sequencing and analysis of microbial communities in the mangrove swamps along the coast of Beibu Gulf in Guangxi, China. Sci. Rep. *9*, 9377.

Gruber, N., and Sarmiento, J.L. (1997). Global patterns of marine nitrogen fixation and denitrification. Glob.Biogeochem. Cycles *11*, 235–266.

Hamilton, S.E. (2020). Assessing 50 Years of Mangrove Forest Loss along the Pacific Coast of Ecuador: A Remote Sensing Synthesis. Coastal Research Library (Springer), pp. 111–137.

Hamilton, S.E., and Lovette, J. (2015). Ecuador's mangrove forest carbon stocks: a spatiotemporal analysis of living carbon holdings and their depletion since the advent of commercial aquacultureB. Ruttenberg, ed. *10*, e0118880.

Holguin, G., Gonzalez-Zamorano, P., de-Bashan, L.E., Mendoza, R., Amador, E., and Bashan, Y. (2006). Mangrove health in an arid environment encroached by urban development-a case study. Sci. Total Environ. *363* (1–3), 260–274.

Holguin, G., Guzman, M.A., and Bashan, Y. (1992). Two new nitrogen-fixing bacteria from the rhizosphere of mangrove trees: their isolation, identification and in vitro interaction with

rhizosphere *Staphylococcus* sp. FEMS Microbiol. Lett. *101* (3), 207–216.

Holguin, G., Vazquez, P., and Bashan, Y. (2001). The role of sediment microorganisms in the productivity, conservation, and rehabilitation of mangrove ecosystems: an overview. Biol. Fertil. Soils *33*, 265–278.

Imchen, M., Kumavath, R., Barh, D., Avezedo, V., Ghosh, P., Viana, M., and Wattam, A.R. (2017). Searching for signatures across microbial communities: metagenomic analysis of soil samples from mangrove and other ecosystems. Sci. Rep. *7*, 1–13.

Jang, G.I., Cho, Y., and Cho, B.C. (2013). Pontimonas salivibrio gen. nov., sp. nov., a new member of the family Microbacteriaceae isolated from a seawater reservoir of a solar saltern. Int. J. Syst. Evol.Microbiol. *63*, 2124–2131.

Jones, H.J., Kröber, E., Stephenson, J., Mausz, M.A., Jameson, E., Millard, A., Purdy, K.J., and Chen, Y. (2019). A new family of uncultivated bacteria involved in methanogenesis from the ubiquitous osmolyte glycine betaine in coastal saltmarsh sediments. Microbiome *7*, 1–11.

Kathiresan, K., and Bingham, B.L. (2001). Biology of mangroves and mangrove ecosystems. Adv. Mar. Biol. *40*, 81–251.

Kulichevskaya, I.S., Ivanova, A.O., Baulina, O.I., Bodelier, P.L., Damsté, J.S., and Dedysh, S.N. (2008). Singulisphaera acidiphila gen. nov., sp. nov., a non-filamentous, Isosphaera-like planctomycete from acidic northern wetlands. Int. J. Syst. Evol.Microbiol. *58*, 1186–1193.

Liu, M., Huang, H., Bao, S., and Tong, Y. (2019). Microbial community structure of soils in Bamenwan mangrove wetland. Sci. Rep. *9*, 8406.

Lønborg, C., Carreira, C., Jickells, T., and Álvarez-Salgado, X.A. (2020). Impacts of global change on ocean dissolved organic carbon (DOC) cycling. Front. Mar. Sci. *7*, 466.

Lovelock, C.E., Feller, I.C., Mckee, K.L., Engelbrecht, B.M.J., and Ball, M.C. (2004). The effect of nutrient enrichment on growth, photosynthesis and hydraulic conductance of dwarf mangroves in Panamá. Funct. Ecol. *18*, 25–33.

Maher, D.T., Sippo, J.Z., Tait, D.R., Holloway, C., and Santos, I.R. (2016). Pristine mangrove creek waters are a sink of nitrous oxide. Sci. Rep. *6*, 25701.

Mohd-Nor, D., Ramli, N., Sharuddin, S.S., Hassan, M.A., Mustapha, N.A., Amran, A., Sakai, K., Shirai, Y., and Maeda, T. (2018). Alcaligenaceae and Chromatiaceae as reliable bioindicators present in palm oil mill effluent final discharge treated by different biotreatment processes. Ecol. Indicators *95*, 468–473.

Mohr, K.I., Garcia, R.O., Gerth, K., Irschik, H., and Müller, R. (2012). Sandaracinus amylolyticus gen. nov., sp. nov., a starch-degrading soil myxobacterium, and description of Sandaracinaceae fam. nov. Int. J. Syst. Evol.Microbiol. *62*, 1191–1198.

Reef, R., Feller, I.C., and Lovelock, C.E. (2010). Nutrition of mangroves. Tree Physiol. *30*, 1148–1160.

Reis, C.R.G., Nardoto, G.B., and Oliveira, R.S. (2017). Global overview on nitrogen dynamics in mangroves and consequences of increasing nitrogen availability for these systems. Plant and Soil *410*, 1–19.

Robertson, A.I., Alongi, D.M., and Boto, K.G. (2011). Food Chains and Carbon Fluxes (American Geophysical Union (AGU)), pp. 293–326.

Robertson, A.I., and Phillips, M.J. (1995). Mangroves as filters of shrimp pond effluent: predictions and biogeochemical research needs. Hydrobiologia *295*, 311–321.

Rosentreter, J.A., Maher, D.T., Erler, D.V., Murray, R.H., and Eyre, B.D. (2018). 'Methane emissions partially offset "blue carbon" burial in mangroves'. Sci. Adv. *4*, eaao4985.

Rubio-Portillo, E., Santos, F., Martínez-García, M., de Los Ríos, A., Ascaso, C., Souza-Egipsy, V., Ramos-Esplá, A.A., and Anton, J. (2016). Structure and temporal dynamics of the bacterial communities associated to microhabitats of the coral *O culina patagonica*. Environ.Microbiol. *18*, 4564–4578.

Salvà-Serra, F., Jakobsson, H.E., Busquets, A., Gomila, M., Jaén-Luchoro, D., Seguí, C., Aliaga-Lozano, F., García-Valdés, E., Lalucat, J., Moore, E.R., and Bennasar-Figueras, A. (2017). Genome sequences of two naphthalene-degrading strains of Pseudomonas balearica, isolated from polluted marine sediment and from an oil refinery site. Genome Announc *5*, e00116–e00117.

Santoro, A.E., Dupont, C.L., Richter, R.A., Craig, M.T., Carini, P., McIlvin, M.R., Yang, Y., Orsi, W.D., Moran, D.M., and Saito, M.A. (2015). 'Genomic and proteomic characterization of "*Candidatus*Nitrosopelagicus brevis": an ammonia-oxidizing archaeon from the open ocean'. Proc. Natl. Acad. Sci. USA *112*, 1173–1178.

Sargent, E.C., Hitchcock, A., Johansson, S.A., Langlois, R., Moore, C.M., LaRoche, J., Poulton, A.J., and Bibby, T.S. (2016). Evidence for polyploidy in the globally important diazotroph Trichodesmium. FEMS Microbiol.Lett. *363*, 244.

Scott, J.J., Budsberg, K.J., Suen, G., Wixon, D.L., Balser, T.C., and Currie, C.R. (2010). Microbial community structure of leaf-cutter ant fungus gardens and refuse dumpsC.-H. Yang, ed. *5*, e9922.

Shiau, Y.J., and Chiu, C.Y. (2020). Biogeochemical processes of C and N in the soil of mangrove forest ecosystems. Forests *11*, 492.

Simon, M., Scheuner, C., Meier-Kolthoff, J.P., Brinkhoff, T., Wagner-Döbler, I., Ulbrich, M., Klenk, H.P., Schomburg, D., Petersen, J., and Göker, M. (2017). Phylogenomics of Rhodobacteraceae reveals evolutionary adaptation to marine and non-marine habitats. ISME J. *11*, 1483–1499.

Sriswasdi, S., Yang, C.C., and Iwasaki, W. (2017). Generalist species drive microbial dispersion and evolution. Nat. Commun. *8*, 1–8.

Vazquez, P., Holguin, G., Puente, M.E., Lopez-Cortes, A., and Bashan, Y. (2000). Phosphate-solubilizing microorganisms associated with the rhizosphere of mangroves in a semiarid coastal lagoon. Biol. Fertil. Soils *30*, 460–468.

Willis, A., and Woodhouse, J.N. (2020). 'Defining cyanobacterial species: diversity and description through genomics. Crit. Rev. Plant Sci. *39*, 101–124.

Yeoh, Y.K., Sekiguchi, Y., Parks, D.H., and Hugenholtz, P. (2016). Comparative genomics of candidate phylum TM6 suggests that parasitism is widespread and ancestral in this lineage. Mol. Biol. Evol. *33*, 915–927.

Zecher, K., Hayes, K.R., and Philipp, B. (2020). Evidence of interdomain ammonium cross-feeding from methylamine- and Glycine betaine-degrading Rhodobacteraceae to diatoms as a widespread interaction in the marine phycosphere. Front.Microbiol. *11*, 533894.

Zhang, C.J., Pan, J., Duan, C.H., Wang, Y.M., Liu, Y., Sun, J., Zhou, H.C., Song, X., and Li, M. (2019). Prokaryotic diversity in mangrove sediments across southeastern China fundamentally differs from that in other biomes. mSystems *4*, e00442-19.

Zhang, Y., Yang, Q., Ling, J., Van Nostrand, J.D., Shi, Z., Zhou, J., and Dong, J. (2017). Diversity and structure of diazotrophic communities in mangrove rhizosphere ,revealed by high-throughput sequencing. Front.Microbiol. *8*, 2032.
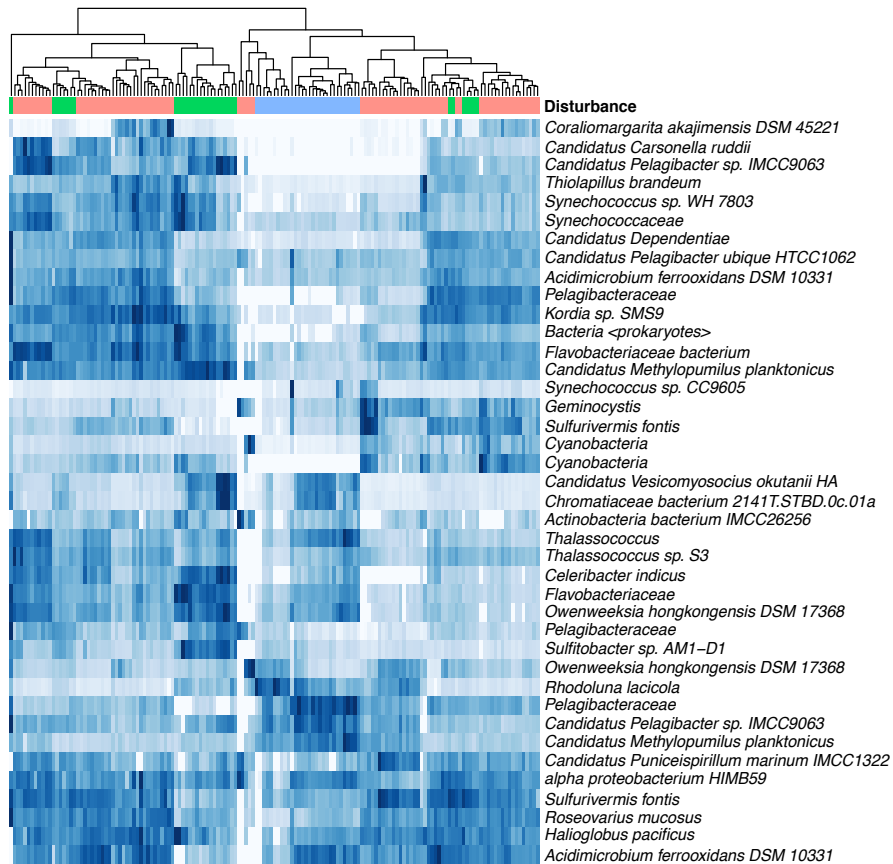
Supplemental information

Sensitivity of the mangrove-estuarine

microbial community

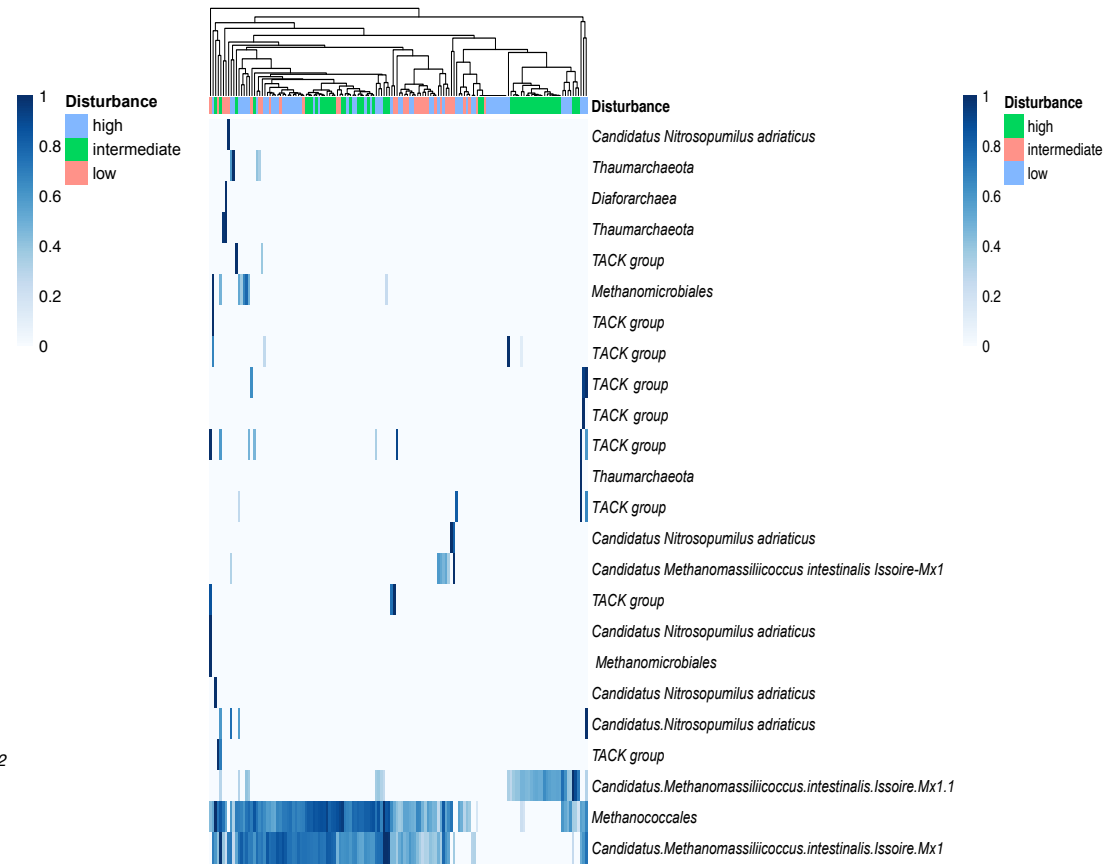# to aquaculture effluent

Natalia G. Erazo and Jeff S. Bowman

Figure S1. Top abundant microbial community (bacteria and archaea). Heatmap for the most abundant bacteria (A) and archaea (B) taxa. Samples were clustered using Bray-Curtis dissimilarity distance and normalized (Hellinger transformation) abundance. Related to Figure 4.
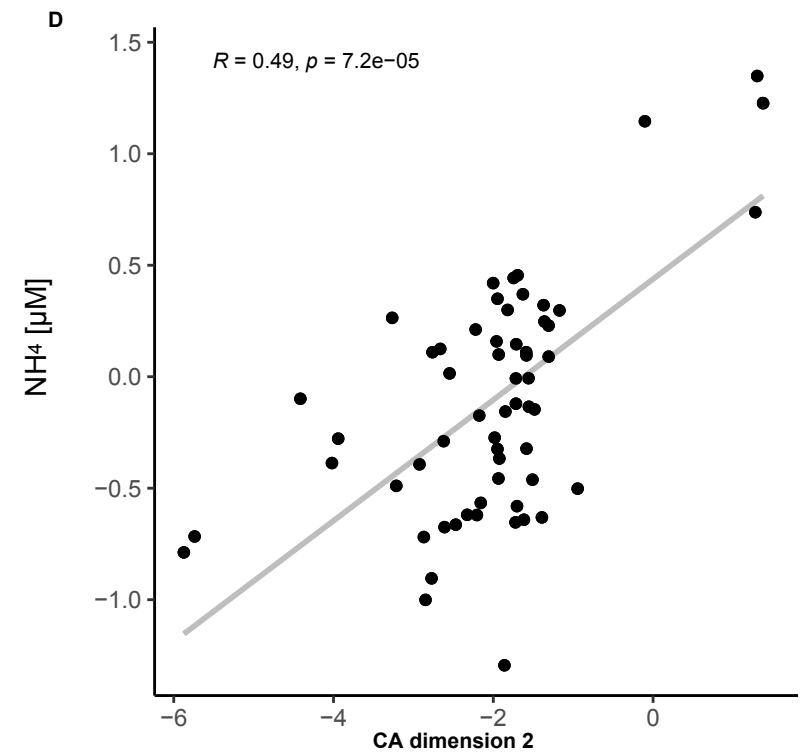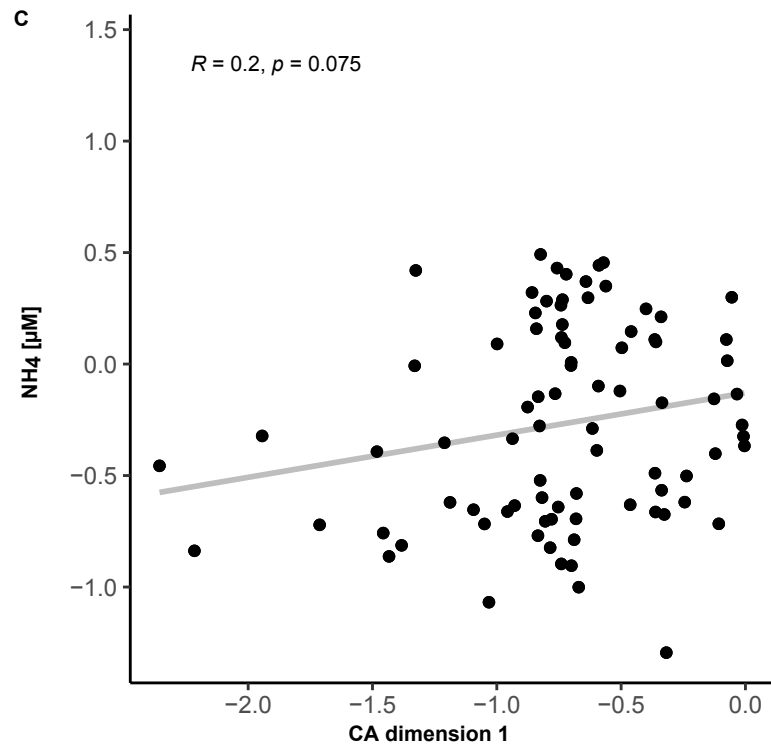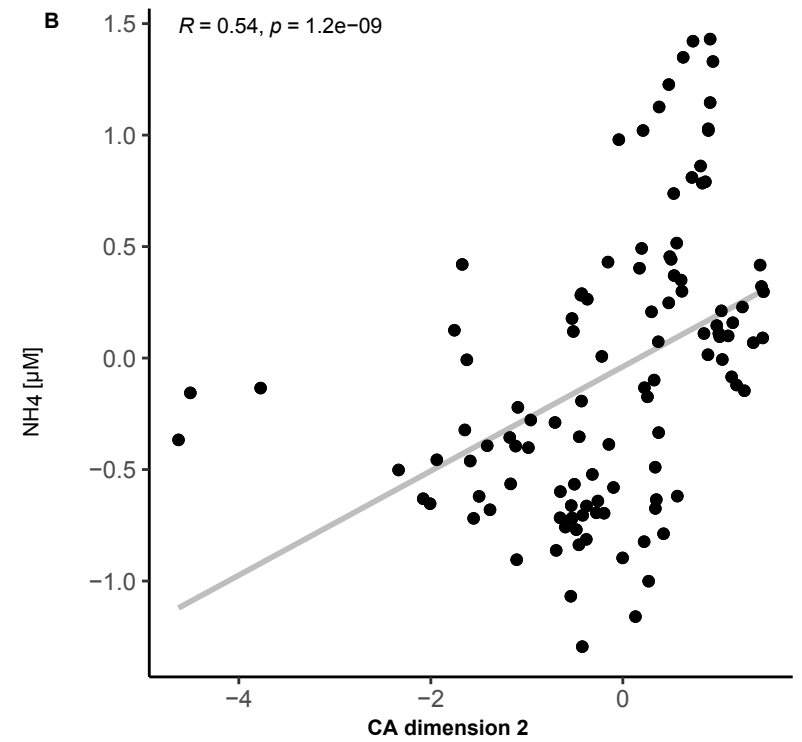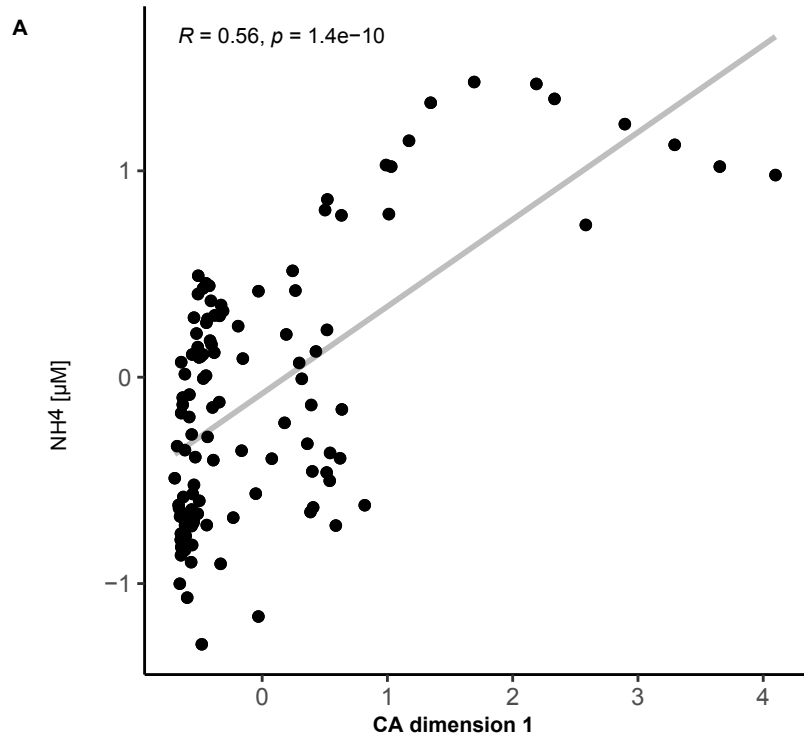
Figure S2. Microbial community structure and association to disturbance levels. CA dimension 1 and dimension 2 vs ammonia concentrations for bacteria (A, B) and for archaea (C, D) (Spearman correlation). Related to Figure 5.
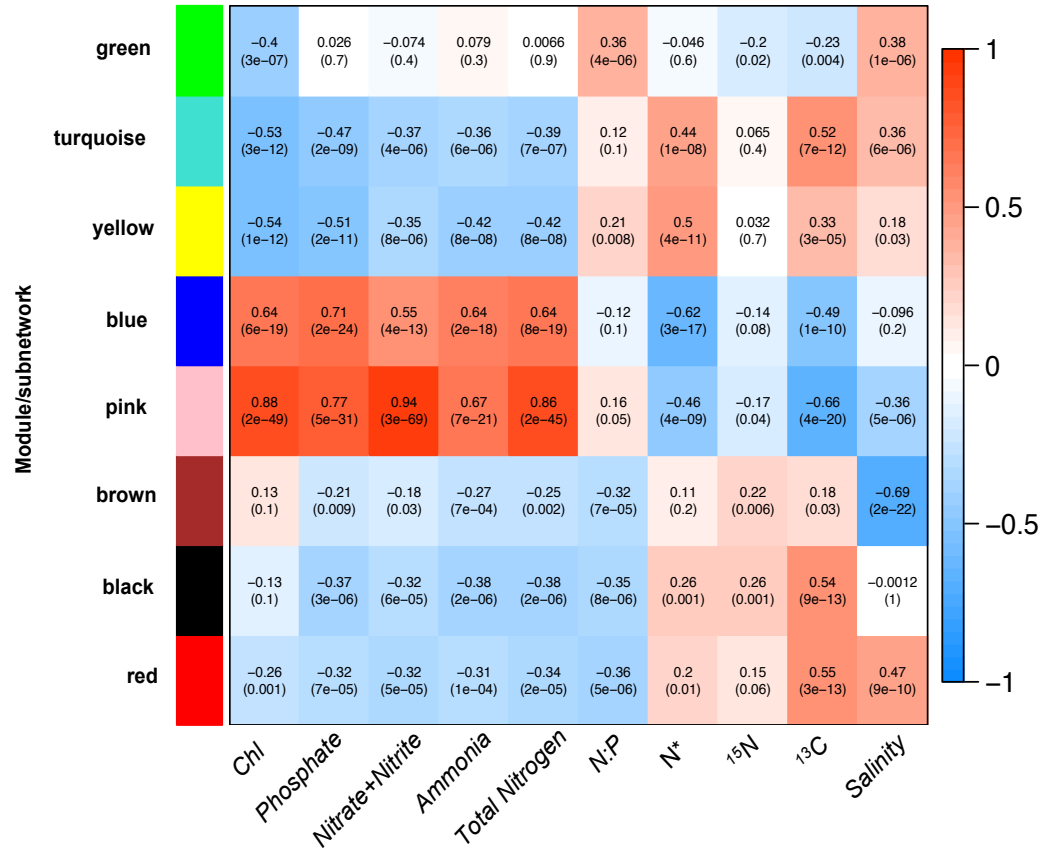
# Module–trait relationships

Figure S3. Microbial community and environmental variables. Weighted Gene Correlation Network Analysis (WGCNA) was used to identify subnetworks (or modules) of bacteria that correlated with environmental variables. Pearson correlation coefficients for subnetworks that were significantly correlated with environmental variables are shown in the top number (ρ value) and the number in the parentheses is the p-value for each relationship. Positive relationship is in red and negative relationship is in blue. Related to Table 2 & 3.
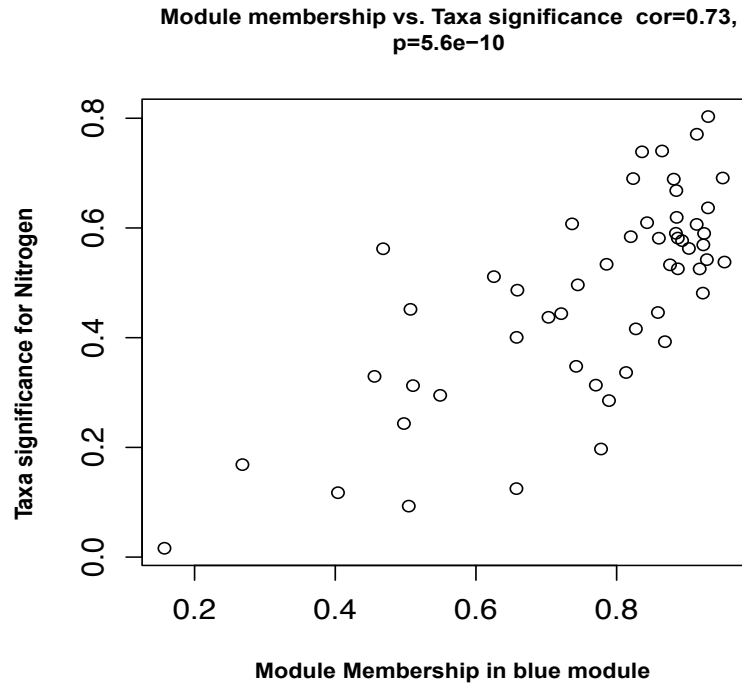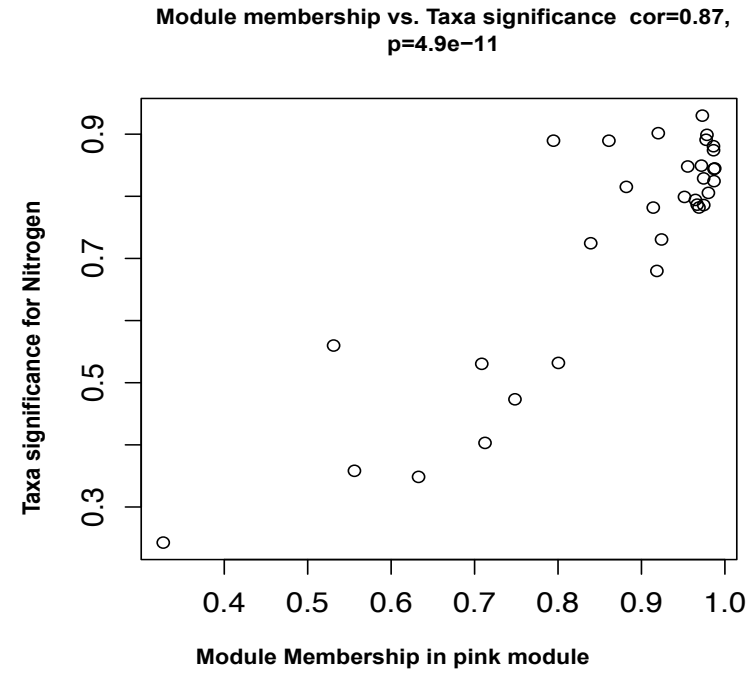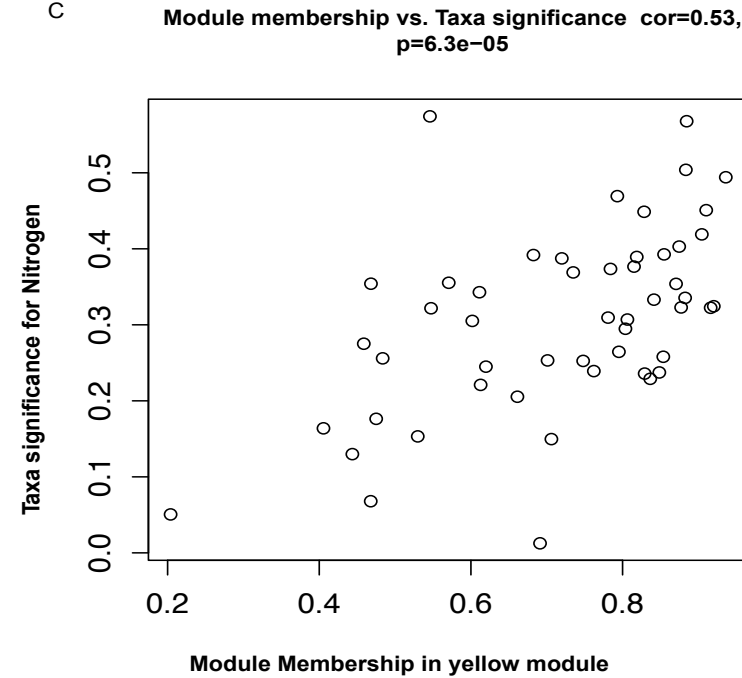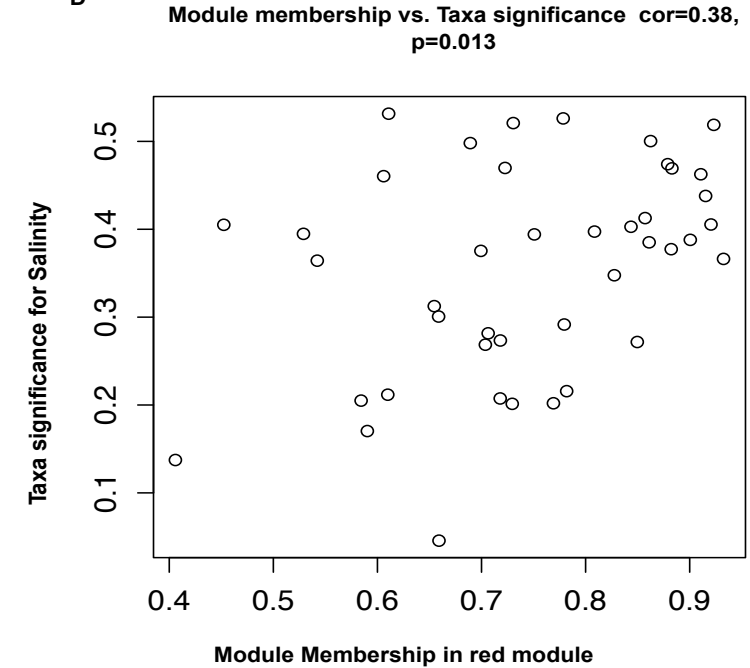
Figure S4. WGCNA modules. Module membership of taxa in the blue (A), pink (B) and yellow (C) subnetworks (or modules) which strongly correlated with ammonia and nitrate + nitrite. Module membership of taxa in red subnetwork (D) which strongly correlated with salinity. Related to Table 2 & 3.
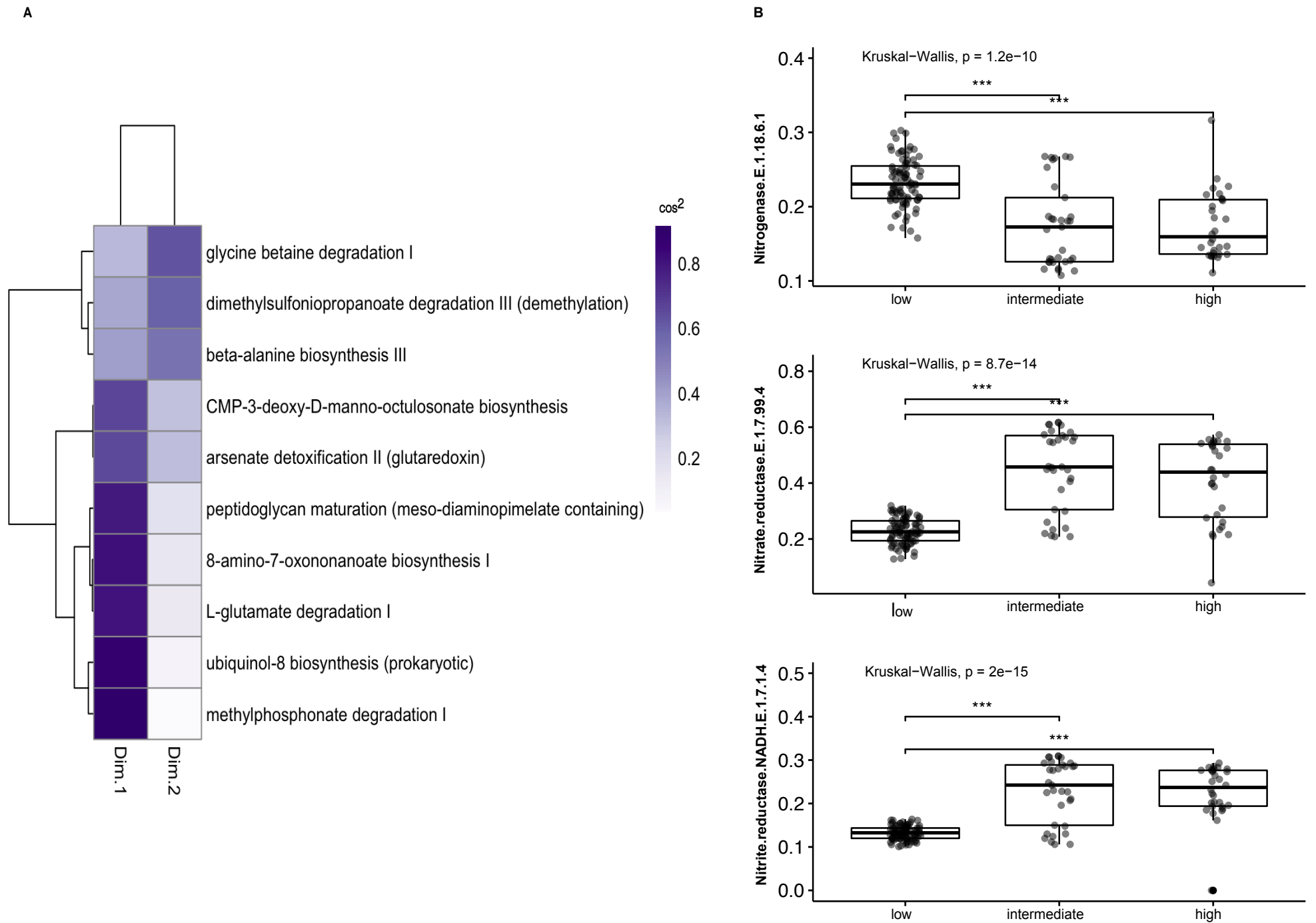
Figure S5. Metabolic pathways. (A) Contribution of top taxa from CCA ordination analysis and cos2 values. (B) Nitrogenase EC 1.18.6.1, Nitrate reductase EC 1.7.99.4 and Nitrite reductase NADH EC 1.7.1.4 normalized (Hellinger transformation) abundance. Kruskal-Wallis test and p-values with Dunn post-test, ***denotes p-value<0.001. Related to Figure 6.

1

Supplementary Information

Transparent Methods

4

Study sites, sample collection, and physiochemical parameter measurements

The study was conducted in two ecological reserves along the coast of Ecuador **(Fig. 1).** The Cayapas-Mataje Ecological Reserve, located within Esmeraldas province along the Colombian border (1° 17' 02.14'' N, 78° 54' 22.29'' W), encompasses 302.05 km^2 of largely non-disturbed mangrove forests. This reserve is located in the delta formed by the estuary of the Cayapas-Santiago-Mataje rivers, and it is part of what used to be a continuous mangrove belt that ranged from the central area of the Colombia Pacific coast to the south area of Esmeraldas in Ecuador. Cayapas-Mataje is considered one of the most pristine mangrove ecosystems along the Pacific coast of the Americas (Hamilton, 2020a). The dominant mangrove species is *Rhizophora mangle*, representing 98% of all the mangrove area (Hamilton, 2020a). Traditional uses, such as artisanal fishing and cockle picking are still practiced, and only 2% of mangrove forest area loss is attributed to aquaculture (Hamilton, 2020b).

The Muisne Ecological Reserve, also located in the province of Esmeraldas (0° 36' 41.81'' N, −80° 1' 14.36'' W), is highly perturbed by aquaculture **(Fig. 1)**. The site compromises the delta of the Muisne River and numerous smaller rivers and contains a total of 12.06 km^2 of mangrove forests. The species composition is 71% *Rhizophora mangle*, 1% *Avicennia germinans*, and 28% *Languncularia racemose* (Hamilton, 2020a). Muisne has been severely impacted by shrimp aquaculture, accounting for 36% of mangrove loss. Only 1% of the remaining mangrove forest is protected (Hamilton, 2020b).

24   Water samples were taken from the surface (0.5 m depth) along a proximity gradient to the

25   mangrove trees. Samples were grouped by level of disturbance based on the concentration of

26   ammonia in the water column: Low = < 1 µM, Intermediate = 1 – 3 µM, High = > 3 µM. Similar

27   ammonia ranges have been identified in previous studies exposed to aquaculture effluent

28   (Robertson and Alongi, 1992); however, reported values in the literature can vary depending on

29   spatial parameters and aquaculture land expansion (Cifuentes *et al.*, 1996; Barraza-Guardado *et*

30   *al.*, 2013a, Samocha *et al.*, 2004). Here we also take into account the area of shrimp aquaculture

31   in the two ecological sites. Muisne was identified as highly disturbed, and all the samples were

32   taken near shrimp aquaculture facilities (N = 29) with high levels of ammonia with the exception

33   of two samples near the mouth of the estuarine. The site has 20.47 km^2 of shrimp farms and 12.06

34   km^2 of mangrove forests for an approximate 2:1 ratio of aquaculture to mangrove forest (Hamilton,

35   2020b). Cayapas-Mataje has 11.04 km^2 of shrimp aquaculture farms and 302.05 km^2 of mangrove

36   forest for a 1:27 ratio of aquaculture to mangrove forest **(Fig. 1)** (Hamilton, 2020b). Thus, samples

37   that were collected along mangrove forests in Cayapas-Mataje (no presence of aquaculture) were

38   characterized as a low disturbance with lower levels of ammonia, and we included one sample

39   from Muisne with low level of ammonia (N = 89). Within Cayapas-Mataje, there's a smaller

40   presence of shrimp aquaculture facilities and the samples that were collected near the shrimp

41   facilities were classified as intermediate disturbance with intermediate levels of ammonia in

42   addition to one sample from Muisne with intermediate ammonia (N = 34).

43   For DNA samples, approximately 400 ml of water was filtered through a sterile 47 mm 0.2

44   µm Supor filter (Pall) directly from 0.5 m depth using a peristaltic pump. The filter was

45   immediately stored on ice and transferred to long term storage at –80 °C within 8 hours.

46   Chlorophyll *a* concentration was measured with an Aquaflash handheld active fluorometer (Turner

47 Designs) following the manufacturer's instructions. Temperature, salinity, and turbidity were

48 measured using a YSI ProDss (Xylem).

49   For nutrient analysis, 50 ml of water was filtered through a combusted GF/F filter (Whatman),

50 frozen immediately after collection, and stored at –80 °C. Samples were sent to the UC Santa

51 Barbara Marine Institute and analyzed by flow injection analysis following standard protocols (

52 Lachat instrument methods: 31-107-04-1A, 31-107-06-5A, 31-115-01-3A). For CHN and isotope

53 analysis, 50 ml of water was filtered through a combusted GF/F filter, and filters were wrapped

54 into a tin envelope (Costech). Samples were analyzed by EA-IRMS at the Scripps Institute of

55 Oceanography Isotope Facility yielding percent carbon and nitrogen by mass, as well as $\delta^{13}C$ and

56 $\delta^{15}N$ following standard methods (Pestle, Crowley and Weirauch, 2014). The reference materials

57 used were NBS-19 and NBS-18, and IAEA N1 and the analytical precisions were +/- 0.3 to 0.5

58 for C and 0.7 to 1.0 for N. The standards used for $\delta^{13}C$ and $\delta^{15}N$ calculations were the Pee Dee

59 Belemnite and atmospheric N_2, respectively.

60 **DNA extraction and sequencing**

61   DNA was extracted using the DNAeasy PowerWater DNA extraction kit (Qiagen). Extracted

62 DNA was quantified using the Qubit HS DNA quantification kit (Invitrogen) and then quality

63 checked by gel electrophoresis and PCR amplification of the 16S rRNA gene using primers 515F

64 and 806R (Walters *et al.*, 2015) for bacteria and archaea. High quality extracted DNA was

65 submitted to the Argonne National Laboratory sequencing center for amplification and library

66 preparation with the same primer set, followed by 2 x 151 paired-end sequenced on the Illumina

67 Miseq platform. Sequences were submitted to NCBI Bio project accession number:

68 PRJNA633714.

Sequence analysis

Illumina Miseq reads were demultiplexed using the 'iu-demultiplex' command in Illumina utils. Demultiplexed reads were quality controlled and denoised using the 'FilterandTrim' and 'dada' commands within the R package dada2 (Benjamin J Callahan *et al.*, 2016), and assembled with the 'mergePairs' command. The final merged reads had mean quality scores >30, and the non-redundant fasta files of the generated unique reads produced by dada2 were used as an input for the paprica pipeline for microbial community structure and metabolic inference (https://github.com/bowmanjeffs/paprica). The paprica method for determining microbial community structure differs from OTU clustering methods in that it relies on the placement of reads on a phylogenetic tree created from the 16S rRNA gene reads from all completed bacterial and archaeal genomes in Genbank (Bowman and Ducklow, 2015). Because the metabolic potential of each phylogenetic edge on the reference tree is known, paprica generates a reasonable estimate of genome sizes, gene content, and metabolic pathways for the organisms of origin of each read. To estimate metabolic potential, a phylogenetic tree of the 16S rRNA genes from each completed genome was generated. For each internal node on the reference tree we determined a "consensus genome", defined as all genomes shared by all members of the clade originating from the node, and predict the metabolic pathways present in the consensus and complete genomes (Bowman and Ducklow, 2015). Unique sequences (referred to as amplicon sequence variants or ASVs) and estimated gene abundances were normalized according to predicted 16S rRNA gene copy number prior to downstream analysis. The paprica community structure results are described in terms of closest estimated genomes (CEGs; for phylogenetic placements to non-terminal edges) and closest completed genomes (CCGs; for placements to terminal edges). CCGs are names according to their

91   lowest consensus taxonomic ranking, while CEGs are named according to their closest relative on

92   the phylogenetic reference tree.

93   **Diversity and statistics analysis**

94   The alpha diversity index, inverse of Simpson, for ASVs was calculated using the phyloseq

95   package in R (McMurdie and Holmes, 2013) following methods described in Callahan (Ben J.

96   Callahan *et al.*, 2016). Kruskal-Wallis tests were performed to test differences among groups in

97   the vegan package in R (Oksanen *et al.*, 2019). For the biogeochemical parameters, we used the

98   Kruskal-Wallis test to test differences among groups, and the Spearman correlation to evaluate

99   relationships between N:P ratio, genome size, and 16S rRNA gene copy number. We determined

100   N* in disturbed and less disturbed sites; this is a measure of nitrogen vs. phosphorus availability

101   based on the Redfield ratio (N:P = 16:1) (Gruber and Sarmiento, 1997), and we calculated based

102   on nutrient concentrations using the following equation (Wilson, Abboud and Beman, 2017):

103

104   (1): $N* = (NO_3^- + NO_2^- + NH_4^+) - 16 \times PO_4^{3-}$

105

106   We used correspondence analysis (CA) to quantify taxon contributions to the sample ordination.

107   This method allowed us to determine the degree of correspondence between sites and species, and

108   which taxa were associated with gradients of disturbance. We performed CA on Hellinger-

109   transformed data such that each value represents a contribution to the Pearson's χ^2 (chi-squared)

110   statistic computed for the data (Legendre P., 1998). We also calculated a $\cos^2$ value that describes

111   the contribution of each taxa to the major axes of disturbance (Kuramae *et al.*, 2012). Analysis of

112   similarity (ANOSIM) was used to assess significant differences with respect to level of

113   disturbance. This nonparametric permutation procedure uses the rank similarity matrix underlying

114 an ordination plot to calculate an *R* test statistic, and it was calculated using the vegan package in

115 R (Oksanen *et al.*, 2019). We examined association of levels of disturbance by a Spearman

116 correlation between ammonia concentrations and dimensions 1 and 2 of CA analysis. To examine

117 the impact of environmental variables associated to aquaculture outflow on the estimated

118 metabolic pathways we performed a canonical correspondence analysis (CCA) to the metabolic

119 output generated in paprica to restrict the sample ordination to nitrogen, phosphate, and isotopic

120 signals to better understand the impact of aquaculture outflow on microbial metabolic potential.

121 The cos^2 value was used to determine the contribution of key metabolic pathways to the major

122 axis. The ordinations were performed in R using the factoMiner and CA package (Husson *et al.*,

123 2020).

124　　　To identify unique reads differentially present between disturbed and non-disturbed sites

125 we used DESeq2 (Michael I Love, Huber and Anders, 2014), following the methods of Webb et

126 al. (2019).   DESeq2 performs differential abundance analysis based on the negative

127 binomial/Gamma-Poisson distribution. The default settings were used, which estimates size

128 factors with the median ratio method (Michael I. Love, Huber and Anders, 2014), followed by

129 estimation of dispersion. Next, a Wald test for generalized linear model coefficients was used to

130 test for significance of coefficients, considering size factors and dispersion. The p-values were

131 attained by the Wald test and corrected for multiple testing using the Benjamini and Hochberg

132 method (Michael I. Love, Huber and Anders, 2014). The most abundant bacterial and archaeal

133 taxa that were significantly differentially present were further examined to identify potential

134 microbial markers of shrimp aquaculture effluent. To determine the role of differentially abundant

135 microbes in nutrient cycling, we utilized the BioCyc database (Karp *et al.*, 2019) in combination

136 with the paprica output to assess the potential for genes coding enzymes associated with nitrogen

137   fixation and denitrification. Enzymes included with our assessment included: nitrogenase; EC

138   1.18.6.1, EC 1,19.6.1, nitrate reductase; EC 17.99.4, EC 1.7.1.1, EC 1.7.1.2, EC 1.9.6.1, EC

139   1.7.2.2, and nitrite reductase; EC1.7.2.1, EC 1.7.2.2, EC 1.7.1.4.

140   To identify modules of highly correlated taxa we used Weighted Gene Correlation Network

141   Analysis (WGCNA) (Langfelder and Horvath, 2008), following the methods of Wilson et al.

142   (2018). A signed adjacency measure for each pair of features (unique reads) was calculated by

143   raising the absolute value of their Pearson correlation coefficient to the power of parameter p. The

144   value $p = 8$ was used for each global network to optimize the scale-free topology network fit. This

145   power allows the weighted correlation network to show a scale free topology where key nodes are

146   highly connected with others. The obtained adjacency matrix was then used to calculate the

147   topological overlap measure (TOM), which, for each pair of features, considers their weighted

148   pairwise correlation (direct relationships) and their weighted correlations with other features in the

149   network (indirect relationships). For identifying subnetworks or 'modules' a hierarchical

150   clustering was performed using a distance based on the TOM measure. This resulted in the

151   definition of several subnetworks, each represented by its first principal component. A subnetwork

152   is the association between the subnetworks and a given trait that is measured by the pairwise

153   relationships (correlations) between the taxa. To find correlations between subnetworks and

154   environmental factors, Pearson's correlation coefficients were calculated between the considered

155   environmental factor and the respective principal components. P-values were adjusted using

156   Bonferroni method. All procedures were applied to Hellinger-transformed abundances.

157

158

159

References

Barraza-Guardado, R. H. *et al.* (2013) 'Effluents of shrimp farms and its influence on the coastal ecosystems of Bahía de Kino, Mexico.', *TheScientificWorldJournal*, 2013, p. 306370.

Bowman, J. S. and Ducklow, H. W. (2015) 'Microbial Communities Can Be Described by Metabolic Structure: A General Framework and Application to a Seasonally Variable, Depth-Stratified Microbial Community from the Coastal West Antarctic Peninsula', *PLOS ONE*. Edited by C. Moissl-Eichinger, 10(8), p. e0135868.

Callahan, Ben J. *et al.* (2016) 'Bioconductor workflow for microbiome data analysis: From raw reads to community analyses [version 1; referees: 3 approved]', *F1000Research*, 5.

Callahan, Benjamin J *et al.* (2016) 'DADA2: High-resolution sample inference from Illumina amplicon data.', *Nature methods*, 13(7), pp. 581–3.

Cifuentes, L. A. *et al.* (1996) 'Isotopic and Elemental Variations of Carbon and Nitrogen in a Mangrove Estuary', *Estuarine, Coastal and Shelf Science*, 43(6), pp. 781–800.

Gruber, N. and Sarmiento, J. L. (1997) 'Global patterns of marine nitrogen fixation and denitrification', *Global Biogeochemical Cycles*, 11(2), pp. 235–266.

Hamilton, S. E. (2020a) 'Introduction to Coastal Ecuador', in *Coastal Research Library*. Springer, pp. 69–110.

Hamilton, S. E. (2020b) 'Assessing 50 Years of Mangrove Forest Loss Along the Pacific Coast of Ecuador: A Remote Sensing Synthesis', in *Coastal Research Library*. Springer, pp. 111–137.

Husson, F. *et al.* (2020) *Package 'FactoMineR' Title Multivariate Exploratory Data Analysis and Data Mining*. [Online] Available at: http://factominer.free.fr

Karp, P. D. *et al.* (2019) 'The BioCyc collection of microbial genomes and metabolic pathways', 20(4), pp. 1085–1093.

Kuramae, E. E. *et al.* (2012) 'Soil characteristics more strongly influence soil bacterial communities than land-use type', *FEMS Microbiology Ecology*, 79(1), pp. 12–24.

Langfelder, P. and Horvath, S. (2008) 'WGCNA: an R package for weighted correlation network analysis.', *BMC bioinformatics*, 9, p. 559.

Legendre P., L. L. F. J. (1998) *Numerical Ecology, Volume 24 - 2nd Edition*, *Elsevier Science*.

Love, Michael I, Huber, W. and Anders, S. (2014) 'Moderated estimation of fold change and dispersion for RNA-seq data with DESeq2', *Genome Biology*, 15(12), p. 550.

McMurdie, P. J. and Holmes, S. (2013) 'phyloseq: An R Package for Reproducible Interactive

Analysis and Graphics of Microbiome Census Data', *PLoS ONE*. Edited by M. Watson, 8(4), p. e61217.

Oksanen, J. *et al.* (2019) *Package 'vegan' Title Community Ecology Package Version 2.0-8*. [Online] Available at: http://CRAN.R-project.org/package=vegan

Pestle, W. J., Crowley, B. E. and Weirauch, M. T. (2014) 'Quantifying Inter-Laboratory Variability in Stable Isotope Analysis of Ancient Skeletal Remains', *PLoS ONE*. Edited by L. Bondioli, 9(7), p. e102844.

Robertson, A. I. and Alongi, D. M. (eds) (1992) *Tropical Mangrove Ecosystems*. Washington, D. C.: American Geophysical Union (Coastal and Estuarine Studies).

Samocha, T. M. *et al.* (2004) 'Characterization of intake and effluent waters from intensive and semi-intensive shrimp farms in Texas', *Aquaculture Research*, 35(4), pp. 321–339.

Walters, W. *et al.* (2015) 'Transcribed Spacer Marker Gene Primers for Microbial Community Surveys', *mSystems*, 1(1), pp. e0009-15.

Webb, S. J. *et al.* (2019) 'Impacts of *Zostera* eelgrasses on microbial community structure in San Diego coastal waters', *Elem Sci Anth*, 7(1), p. 11.

Wilson, J., Abboud, S. and Beman, J. M. (2017) 'Primary Production, Community Respiration, and Net Community Production along Oxygen and Nutrient Gradients: Environmental Controls and Biogeochemical Feedbacks within and across "Marine Lakes"', *Frontiers in Marine Science*, 4.

Wilson, J. M., Litvin, S. Y. and Beman, J. M. (2018) 'Microbial community networks associated with variations in community respiration rates during upwelling in nearshore Monterey Bay, California', *Environmental Microbiology Reports*, 10(3), pp. 272–282.